HHS Public Access

Author manuscript

Nat Med. Author manuscript; available in PMC 2019 July 01.

Published in final edited form as:

Nat Med. 2019 January ; 25(1): 130–140. doi:10.1038/s41591-018-0262-9.

Wiskott–Aldrich syndrome protein (WASP) is a tumor suppressor in T cell lymphoma

Matteo Menotti[1,14], **Chiara Ambrogio**[2,13], **Taek-Chin Cheong**[3,13], **Chiara Pighi**[1,3], **Ines Mota**[1], **Seth H. Cassel**[4,5,6,7], **Mara Compagno**[1,3], **Qi Wang**[3], **Riccardo Dall'Olio**[1], **Valerio Minero**[1], **Teresa Poggio**[1], **Geeta Geeta Sharma**[8], **Enrico Patrucco**[1], **Cristina Mastini**[1], **Ramesh Choudhari**[1,15], **Achille Pich**[1], **Alberto Zamo'**[9], **Roberto Piva**[1], **Silvia Giliani**[10], **Luca Mologni**[8], **Clayton K. Collings**[4,5], **Cigall Kadoch**[4,5], **Carlo Gambacorti-Passerini**[8], **Luigi D. Notarangelo**[11], **Ines M. Anton**[12], **Claudia Voena**[1,*], and **Roberto Chiarle**[1,3,*]

[1]Department of Molecular Biotechnology and Health Sciences, University of Torino, Torino, Italy

[2]Department of Medical Oncology, Dana-Farber Cancer Institute, Boston, MA, USA

[3]Department of Pathology, Boston Children's Hospital and Harvard Medical School, Boston, MA, USA

[4]Department of Pediatric Oncology, the Dana-Farber Cancer Institute and Harvard Medical School, Boston, MA, USA

[5]The Broad Institute of MIT and Harvard, Cambridge, MA, USA.

[6]Biomedical and Biological Sciences Program, Harvard Medical School, Boston, MA, USA.

[7]Medical Scientist Training Program, Harvard Medical School, Boston, MA, USA.

[8]School of Medicine and Surgery, University of Milan-Bicocca, Monza, Italy

[9]Department of Oncology, University of Torino, Torino, Italy

[10]Nocivelli Institute for Molecular Medicine, Department of Molecular and Translational Medicine, University of Brescia, Italy

[11]Laboratory of Clinical Immunology and Microbiology, National Institute of Allergy and Infectious Diseases, National Institutes of Health, Bethesda, MD

[12]Department of Molecular and Cellular Biology, Centro Nacional de Biotecnología (CNB-CSIC), Madrid, Spain

[*]Correspondence: roberto.chiarle@childrens.harvard.edu, claudia.voena@unito.it.

AUTHOR CONTRIBUTIONS

M.M., C.A., T.-C.C., C.P., I.M., S.H.C., M.C., R.D., T.P., E.P., C.M., C.V. performed experiments; M.M., V.M., C.V., R. Choudhari performed mice experiments; Q.W. and C.K.C. performed bioinformatics analysis; A.P. analyzed data; R.P. provided gene expression data on lymphoma samples; C.K. provided reagents for ChIP-seq; S.G., L.G.N. provided WAS patient samples and analyzed data, G.G.S., L.M., C.G.-P. provided sequencing data on ALCL patients; A.Z. provided lymphoma cases, I.M.A. contributed mouse strains and analyzed data; C.V., R. Chiarle conceived and analyzed the experiments; M.M., C.V., R. Chiarle wrote the manuscript.

DATA AVAILABILITY STATEMENT

Gene Expression Omnibus repository accession number for the gene expression profiling data from WT and WASP$^{-/-}$ mice is GSE102889 (token: gzelisgodjkdxqt); for ChIP-seq data is GSE117164 (token: chupqsgklxivtox). Gene expression profiling data for human T cell lymphoma are deposited with Gene Expression Omnibus repository accession number GSE65823[13].

COMPETING INTERESTS STATEMENT

The Authors have no competing financial interests to declare.

[13]These authors contributed equally: Chiara Ambrogio and Taek-Chin Cheong

[14]Present address: Cell Signalling Group, Cancer Research UK Manchester Institute, The University of Manchester, UK

[15]Present address: Center of Emphasis in Cancer, Paul L. Foster School of Medicine, Department of Biomedical Sciences, Texas Tech University Health Sciences Center, El Paso, TX

Abstract

In T lymphocytes WASP and WIP regulate TCR signaling but their role in lymphoma is largely unknown. Here we show that the expression of WASP and WIP is frequently low or absent in anaplastic large cell lymphoma (ALCL) compared to other T cell lymphomas. In ALK+ ALCL, WASP and WIP expression is regulated by ALK oncogenic activity via its downstream mediators STAT3 and C/EBP-β. ALK+ lymphomas were accelerated in WASP- and WIP-deficient mice. In the absence of WASP, active GTP-bound CDC42 was increased and the genetic deletion of one CDC42 allele was sufficient to impair lymphoma growth. WASP-deficient lymphoma showed increased MAPK pathway activation that could be exploited as a therapeutic vulnerability. Our findings demonstrate that WASP and WIP are tumor suppressors in T cell lymphoma and suggest that MEK inhibitors combined with ALK inhibitors could achieve a more potent therapeutic effect in ALK+ ALCL.

INTRODUCTION

Loss-of-function mutations in the gene *WAS* that encodes the WAS protein (WASP) cause the Wiskott–Aldrich syndrome (WAS), a rare X-linked primary immunodeficiency of variable severity characterized by microthrombocytopenia, eczema, autoimmunity, recurrent infections and predisposition to lymphoma development[1]. Since WASP is selectively expressed in hematopoietic cells, the phenotype in WAS patients is associated with defects in hematopoiesis and the immune system. WASP abundance in cells is regulated by the WASP-interacting protein (WIP). WIP, encoded by the gene *WIPF1*, binds to the WH1 domain of WASP and protects WASP from degradation[2–5]. The main regulator of WASP activation is the Rho family GTPase cell division cycle 42 (CDC42). In its GTP-bound state, CDC42 binds the GTPase-binding domain (GBD) of WASP to release the verprolin homology domain–cofilin homology domain–acidic region (VCA) autoinhibitory domain and to permit the binding to the ARP2/3 complex and actin nucleation[4,6,7]. Additional mediators such as PIP2, and hematopoietic-specific kinases, such as BTK, LTK, FYN, and NCK1 contribute to the activation of WASP[7,8].

T lymphocytes from WAS patients and WASP- and WIP-deficient mice show a number of defects, including defective proliferation in response to T cell receptor (TCR) stimulation, disturbed formation of surface projections, defective cytokine polarization and secretion, disrupted assembly of filamentous actin at the immunological synapse, and impaired TCR-mediated signaling[7–10]. Other cells of the adaptive immune system, such as B cells, as well as cells of the innate immune system such as macrophages and dendritic cells also have functional defects that have yet to be completely characterized[7,11]. Importantly, WASP-

dependent actin nucleation is essential for the formation of the immunological synapses in T cells and several other WASP-mediated phenotypes[4,7].

Increasing evidence support the concept that TCR-mediated signaling is also critical for the pathology of T cell lymphoma. Mutations in genes involved in TCR signaling, such as *KRAS, RHOA, VAV1, CD28, FYN, LCK*, and *PLCG1,* are frequently found in T cell lymphomas that retain TCR expression, such as Peripheral T Cell Lymphoma (PTCL-NOS) and angioimmunoblastic T-cell lymphoma (AITL)[12]. By contrast, in Anaplastic Large Cell Lymphoma (ALCL) TCR signaling is typically lost, and is bypassed by oncogenic tyrosine kinase signaling, most often secondary to aberrant activation of ALK, ROS1 or TYK2[13–16]. Among several pathways downstream the TCR signaling, recent discoveries highlighted the pathogenetic role in T cell lymphoma of Rho GTPases, such as RAC1, CDC42 and RHOA[12]. Inactivating or dominant negative mutations in *RHOA* are the most common recurrent genetic event in AITL and are also present in PTCL-NOS[17–19]. *RAC1* and *CDC42* genes are not recurrently mutated in lymphoma, yet they are activated by mutations of upstream GTP-exchange factors (GEFs), such as *VAV1* and *VAV3*. VAV1 is frequently activated by mutations and translocations in PTCL[20] whereas oncogenic ALK constitutively activates VAV1 and VAV3 in ALCL, thereby increasing RAC1 and CDC42 activity and promoting lymphoma survival[21–23]. Taken together, these studies indicate the critical role of downstream mediators of TCR signaling and Rho GTPases in T cell lymphoma. In this context, in contrast to the well-characterized function of WASP and WIP in normal TCR signaling, their role in T cell lymphoma is largely unknown.

We investigated WASP and WIP expression in a series of T cell lymphomas and found that WASP and WIP expression are selectively low or absent in ALCL but retained in lymphomas with conserved TCR signaling, such as PTCL-NOS and AITL. WASP or WIP deficiency accelerated significantly the development of ALK-driven lymphoma in mice by increasing active CDC42 and enhancing MAPK signaling. Reduction of CDC42 abundance by deletion of one copy of *Cdc42* abrogated the acceleration of lymphomagenesis in WASP-deficient mice. Therapeutically, the forced re-expression of WASP impaired lymphoma growth and MAPK inhibitors potentiated the effect of the ALK inhibitor crizotinib and exposed an enhanced vulnerability in ALK-driven lymphoma. Overall, these results indicate that WASP is a tumor suppressor in ALCL and highlight specific therapeutic susceptibilities.

RESULTS

Selective low expression of WASP and WIP in Anaplastic Large Cell Lymphoma

To investigate the potential role of WASP and WIP in the ontogeny of T cell lymphomas, we analyzed WASP and WIP mRNA expression in a series of human T cell lymphomas including AITL, PTCL-NOS, ALK+ and ALK- ALCL, which altogether account for more than 90% of T cell lymphomas[24]. ALK expression was confined to ALK+ ALCL, *TNFSR8 (CD30)* expression was enriched in ALCL, *WASP*, *CDC42*, *N-WASP* mRNA expression was similar in various subtypes of T cell lymphoma, whereas *WIP* mRNA was significantly lower in ALCL, being lowest in ALK+ALCL (Fig. 1a). Because WIP regulates WASP stability, we investigated the expression of WASP and WIP proteins by immunohistochemistry in a series of T lymphomas. We found that expression of WASP and

WIP was frequently low or negative in ALCL, but it was always retained in AITL and PTCL-NOS as well as in other rare T cell lymphoma such as NK/T cell lymphoma and γδ hepatosplenic T cell lymphoma (Fig. 1b,c and Supplementary Fig. 1a,b). Taken together, these data showed that WASP and WIP expression is selectively decreased in ALCL as compared to other T cell lymphomas.

WASP or WIP deficiencies accelerate T cell lymphoma development

WASP deficient mice do not develop lymphoma spontaneously, have normal T thymic cell maturation, but exhibit defective T cell activation[9]. To address directly the biological role of WASP and WIP in ALCL, we crossed NPM-ALK transgenic mice with *Wasp*$^{-/-}$ mice. The NPM-ALK fusion protein is the canonical and most frequent driver oncogene in ALCL, and *NPM-ALK* transgenic mice develop T cell lymphoma with high penetrance[25]. *NPM-ALK/Wasp*$^{-/-}$ females and *NPM-ALK/Wasp*$^{-}$ males showed similar phenotypes and are collectively referred as to *NPM-ALK/Wasp*$^{-/-}$ mice. As expected, *NPM-ALK/Wasp*$^{-/-}$ mice had a complete lack of WASP (Supplementary Fig. 1c). The number of T cells and the pattern of thymic T cell development were comparable in *NPM-ALK* and *NPM-ALK/Wasp*$^{-/-}$ mice (Supplementary Fig. 1d,e). Remarkably, WASP deficiency significantly accelerated the onset of lymphomas and hastened mortality (Fig. 2a,b). *NPM-ALK/Wasp*$^{+/-}$ female mice had protein abundance comparable to *NPM-ALK/Wasp*$^{+/+}$ mice, and did not show any acceleration in lymphomagenesis (Fig. 2a,b).

Mice with WIP deficiency have impaired T and B cell activation as a result of defects in the subcortical actin filament network. WASP is almost undetectable in *Wip*$^{-/-}$ mice, because WASP stability depends on binding to WIP[2]. Recently, patients with disruptive mutations in *WIP* have been identified. These patients lack expression of both WIP and WASP and present with a clinical phenotype similar to WAS patients[26,27]. Therefore, we reasoned that if the amount of WASP protein is critical for the kinetics of NPM-ALK driven lymphoma, WIP deficiency should accelerate lymphomagenesis in a manner similar to WASP deficiency. Indeed, *NPM-ALK/Wip*$^{-/-}$ mice phenocopied *NPM-ALK/Wasp*$^{-/-}$ mice with regard to the onset of lymphoma. In contrast to *NPM-ALK/Wasp*$^{+/-}$ mice, *NPM-ALK/Wip*$^{+/-}$ mice had a phenotype intermediate between *NPM-ALK/Wip*$^{-/-}$ and *NPM-ALK/Wip*$^{+/+}$ mice (Fig. 2c). When we analyzed the protein levels, as expected *NPM-ALK/Wip*$^{-/-}$ lymphomas had undetectable levels of both WIP and WASP[3] whereas *NPM-ALK/Wip*$^{+/-}$ lymphomas expressed intermediate levels of both WIP and WASP (Fig. 2d). Immunostains for cleaved Caspase 3 and Ki-67 protein demonstrated that the accelerated lymphomagenesis in *NPM-ALK/Wasp*$^{-/-}$ or *NPM-ALK/Wip*$^{-/-}$ mice was associated with reduced apoptosis and increased proliferation of lymphoma cells (Fig. 2e–g). The similarity of the survival phenotype between WASP and WIP deficient mice (Fig. 2a,c) is consistent with the near complete absence of WASP in WIP-deficient mice (Fig. 2d), and is in keeping with the known role of WIP in WASP stability[3]. Heterozygous *Wip*$^{+/-}$ mice had intermediate levels of WASP and WIP expression, as well as an intermediate survival phenotype, indicating that relative levels of WASP can contribute to the kinetics of lymphoma development. Overall, these data suggest that WASP deficiency likely bears responsibility for the phenotype in WIP-deficient mice. These results mirror the findings in human WAS patients, where a complete absence of the protein is associated with a more profound phenotype, including a

higher risk of lymphoma development, compared to patients that retain partial expression of WASP and present with milder phenotypes and a lower incidence of lymphoid malignancies[10,28].

Oncogenic activity of NPM-ALK in lymphocytes controls actin polymerization via a direct activation of VAV1 and VAV3, which are GEFs for RAC1 and CDC42[21,22]. Lymphocytes transformed by NPM-ALK are large and irregular (hence the term “anaplastic” that collectively defines ALK-rearranged lymphoma), hypermotile and have accentuated cellular polarization due to polar assembly of actin filaments[21,23]. Lymphomas that developed in *NPM-ALK/Wasp*$^{-/-}$ or *NPM-ALK/Wip*$^{-/-}$ mice had a significantly smaller mean cellular diameter than NPM-ALK lymphoma cells (Supplementary Fig. 2a,b). *NPM-ALK/Wasp*$^{-/-}$ or *NPM-ALK/Wip*$^{-/-}$ lymphoma cells also showed markedly decreased actin polarization (Supplementary Fig. 2a,c), consistent with defects of actin nucleation and assembly associated with complete loss of WASP or WIP. In reverse experiments, doxycycline-inducible overexpression of WASP and WIP in human ALCL resulted in increased mean cellular diameter and actin polymerization (Supplementary Fig. 2d,e).

CDC42 mediates accelerated lymphoma development in WASP deficient cells

To elucidate the mechanisms of accelerated lymphomagenesis in the absence of WASP, we characterized the expression profiles of *NPM-ALK-Wasp*$^{-/-}$ lymphomas (Supplementary Fig. 3a). Gene Set Enrichment Analysis (GSEA) demonstrated that serum response factor (SRF) pathway, known to be activated by Rho family GTPase signaling[29], as well as other GTPase signatures, were significantly enriched in *NPM-ALK/Wasp*$^{-/-}$ lymphoma compared to *NPM-ALK/Wasp*$^{+/+}$ lymphoma (Supplementary Fig. 3b–d). Since WASP is a critical substrate of GTP-bound CDC42, we reasoned that WASP deficiency could affect CDC42 activity in lymphoma cells resulting in an increased GTPase signature. To explore this possibility, we assessed the abundance of active GTP-bound CDC42 in *NPM-ALK/Wasp*$^{-/-}$ lymphoma. We analyzed *NPM-ALK/Wasp*$^{-/-}$ and *NPM-ALK/Wasp*$^{+/+}$ lymphomas by CDC42-specific GTPase assay. *NPM-ALK/Wasp*$^{-/-}$ lymphomas had significantly higher levels of GTP-bound CDC42 than *NPM-ALK/Wasp*$^{+/+}$ lymphomas (Fig. 3a), indicating that the amount of active CDC42 is increased in cells that lack WASP. In addition to increased CDC42 activation, *NPM-ALK/Wasp*$^{-/-}$ lymphomas also showed increased activation of the MAPK pathway as assessed by ERK½ phosphorylation (Fig. 3b).

To assess directly whether CDC42 abundance was critical for lymphoma acceleration in WASP deficient cells, we crossed *NPM-ALK/Wasp*$^{-/-}$ mice with a conditional *Cdcd42*^{lox} allele; deletion of *Cdc42* in T cells was accomplished by further crossing with *CD4-Cre* mice[23]. The deletion of one *Cdc42* allele was associated with decreased protein abundance (Fig. 3c) and was sufficient to delay lymphoma development in *NPM-ALK/Wasp*$^{-/-}$ (Fig. 3d). Remarkably, lymphoma development and survival of *NPM-ALK/Wasp*$^{-/-}$*/Cdc42*$^{f/+}$*/CD4-Cre* mice was similar to *NPM-ALK/Wasp*$^{+/+}$ mice. *NPM-ALK/Wasp*$^{-/-}$ mice with a complete knockout of *Cdc42* (*NPM-ALK/Wasp*$^{-/-}$*/Cdc42*$^{f/f}$*/CD4-Cre* mice) died prematurely due to multiorgan failure due to an inflammatory infiltrate and the development of lymphoma could not be assessed. Apoptosis was uniformly higher and proliferation consistently lower in *NPM-ALK/Wasp*$^{-/-}$*/Cdc42*$^{f/+}$*/CD4-Cre* lymphomas compared to

NPM-ALK/Wasp$^{-/-}$ lymphomas, but comparable to *NPM-ALK/Wasp*$^{+/+}$ lymphomas (Fig. 3e–g). We concluded that the accelerated lymphomagenesis in *NPM-ALK/Wasp*$^{-/-}$ mice depends on the abundance of CDC42.

To further characterize the role of CDC42 in *NPM-ALK/Wasp*$^{-/-}$ lymphomas, we immortalized lymphoma cell lines of different genotypes and induced *Cdc42* deletion with a tamoxifen-inducible Cre-recombinase. As expected, deletion of one *Cdc42* allele reduced CDC42 protein abundance by approximately 50%, whereas bi-allelic deletion abrogated CDC42 expression (Fig. 4a). Deletion of one *Cdc42* allele significantly impaired the growth of *NPM-ALK/Wasp*$^{-/-}$ lymphoma cells but not of *NPM-ALK/Wasp*$^{+/+}$ lymphoma cells (Fig. 4b), mirroring the results obtained in mice (Fig. 3d) and confirming that CDC42 abundance is critical for *Wasp*$^{-/-}$ lymphoma. Consistently, deletion of one *Cdc42* allele produced an increase in apoptosis in *NPM-ALK/Wasp*$^{-/-}$ lymphomas but not in *NPM-ALK/Wasp*$^{+/+}$ lymphoma cells (Fig. 4c). Consistent with our previous findings[23], in *NPM-ALK/Wasp*$^{+/+}$ lymphoma only the biallelic deletion of *Cdc42* induced impairment of lymphoma growth and apoptosis (Fig. 4c). Altogether, these data demonstrate that WASP-deficient cells are exquisitely sensitive to the cellular abundance of CDC42.

Oncogenic ALK activity promotes WASP and WIP down–regulation via STAT3 and C/EBP-β

To investigate WASP- and WIP-dependent mechanisms of ALK+ ALCL lymphoma progression, we measured WASP and WIP expression in ALK cell lines and confirmed that in several cell lines they were lower compared to normal T cells or other lymphoma types (Fig. 5a and Supplementary Fig. 4a). By contrast, N-WASP was not decreased in ALCL (Supplementary Fig. 5a). *WIP* mRNA was lower in ALK+ ALCL cell lines than in other T cell lines or in T cells from normal donors, whereas *WASP* mRNA was more variable (Fig. 5b). Overall these patterns of gene expression in ALCL cell lines recapitulate the findings in primary ALCL from patients (Fig. 1).

As it is known that ALK oncogenic activity controls protein expression by transcriptional regulation or epigenetic silencing[30,31], we tested whether WASP and WIP expression were directly controlled by ALK activity. Knocking-down *ALK* expression with an inducible shRNA system[32], led to increased *WASP* and *WIP* mRNA and protein expression (Fig. 5c,d). Consistently, inhibition of ALK activity by the ALK inhibitors crizotinib and alectinib resulted in increased *WASP* and *WIP* mRNA expression (Fig. 5e). Conversely, doxycycline-inducible expression of oncogenic ALK in ALK-negative lymphoma cells down-regulated the expression of both WASP and WIP (Supplementary Fig. 5b). Treatment of cells with azacitidine, which is known to restore expression of genes, such as *LAT* and *ZAP70*, that are repressed by ALK through methylation[30,31], did not change WASP and WIP expression (Supplementary Fig. 5c,d). Oncogenic ALK activates several downstream pathways, with STAT3 and C/EBP-β representing key downstream effectors[16]. Knock-down of either *STAT3* or *C/EBP-β* resulted in an increased *WASP* and *WIP* mRNA and protein levels (Fig. 5f and Supplementary Fig. 5e–g). Taken together, these data indicate that ALK oncogenic activity impairs WASP and WIP expression by a transcriptional repression mediated by STAT3 and C/EBP-β. To investigate if STAT3 and C/EBP-β might directly regulate expression of *WAS* and *WIPF1* genes, we performed ChIP-seq on ALCL cell lines treated

with crizotinib. As expected, 3 hours of treatment with crizotinib blocked ALK phosphorylation that in turn resulted in a marked de-phosphorylation of STAT3 without affecting total STAT3 levels (Supplementary Fig. 6a). When ALK was active, STAT3 bound genome-wide, whereas in the presence of crizotinib STAT3 binding was almost completely abrogated throughout the genome (Fig. 5g and Supplementary Fig. 6c), including at loci proximal to both the *WAS* and *WIPF1* genes (Fig. 5h,i). In contrast, C/EBP-β bound to *WAS* and *WIPF1* genes but its binding was not affected by ALK blockade (Fig. 5h,i and Supplementary Fig. 6b,c). Remarkably, STAT3 and C/EBP-β binding sites co-localized with H3K4me3 and H3K27Ac marks indicating that they could functionally contribute to WASP and WIP expression (Supplementary Fig. 6d). Thus, our results are consistent with a model by which STAT3 and C/EBP-β regulate WASP and WIP expression where STAT3 regulation directly depends on an ALK-mediated activation.

WASP and WIP abundance control lymphoma growth

As absence of WASP accelerates lymphoma growth in mouse models, we reasoned that decreased WASP and WIP expression could contribute also to the biology of human ALK+ ALCL. To test this hypothesis, we forcibly re-expressed WASP and WIP in ALCL cells by using a doxycycline-inducible lentiviral vector. Transduction with WASP vector alone did not increase WASP expression (not shown), whereas transduction with WIP lentivirus induced a moderate increase in endogenous WASP (Supplementary Fig. 7a), confirming that the levels of WASP in ALCL are regulated by WIP as they are in normal T cells. When ALCL cells were co-transduced with both WASP and WIP lentiviruses, WASP expression was comparable to normal T cells (Fig. 6a). Upon WASP and WIP induction, the GTP-bound form of CDC42 markedly decreased in ALCL cells, thus confirming that WASP expression level regulates the abundance of active CDC42 also in human ALCL cell lines (Fig. 6b). Next, we found that ALCL cell lines with induced WASP and WIP expression had impaired growth *in vitro* (Supplementary Fig. 7b–d) associated with an increased fraction of cells arrested in G1 phase of the cell cycle (Supplementary Fig. 7e). Consistently, the growth of ALCL mouse xenografts was significantly reduced when WASP and WIP expression was induced *in vivo* (Fig. 6c). Induced expression of WASP in ALCL xenografts was associated with a significant increase in apoptosis and a decrease in proliferation (Fig. 6d,e and Supplementary Fig. 7f). Furthermore, the activation of the MAPK pathway, as measured by phosphorylated ERK½ levels, decreased upon WASP and WIP induction, concomitant with an increase in cleaved Caspase 3 (Supplementary Fig. 4b). Thus, the low expression of WASP and WIP contributes the pathogenesis of ALCL and the restoration of their expression impairs lymphoma growth by decreasing the amount of active CDC42 and MAPK signaling.

MAPK activation is a therapeutic vulnerability in WASP-deficient lymphoma.

Finally, we reasoned that increased MAPK signaling in ALCL cells expressing low levels of WASP could represent a therapeutic vulnerability. To test this concept, we treated lymphoma cells with trametinib, a MEK inhibitor approved for melanoma treatment and currently in trial for lymphoma (NCT00687622). Lymphomas from *NPM-ALK/Wasp*$^{-/-}$ mice were more sensitive than WT lymphoma to trametinib (Fig. 6f) as well as to additional MEK inhibitors (selumetinib, MEK162 and PD0325901) (Supplementary Fig. 8a). Consistently,

human ALCL with low WASP expression (SU-DHL1 and JB6) were also more sensitive than ALCL with higher WASP expression (TS and L82) (Supplementary Fig. 8b). Since ALK inhibitors have potent clinical activity in ALK+ ALCL[16,33], we also investigated whether MEK inhibition could potentiate ALK inhibitors in a combination therapy, as recently suggested for ALK-rearranged lung cancer[34]. *In vitro,* NPM-ALK lymphoma lines were sensitive to crizotinib and the combination with trametinib further potentiated crizotinib activity (Supplementary Fig. 8c). In vivo, trametinib alone did not have an effect against NPM-ALK lymphoma, as expected from similar experiment in ALK+ lung cancer[34]. In contrast, the combination of trametinib with crizotinib was more potent than crizotinib alone for the treatment of *NPM-ALK/Wasp*$^{-/-}$ but not WT lymphoma (Fig. 6g), supporting the concept that the MAPK pathway is a therapeutic vulnerability in WASP-deficient lymphoma.

Lymphocytes from WAS patients show increased CDC42 activity and MAPK signaling

WAS patients have a variety mutations in the *WAS* gene that result in a variably reduce abundance or function WASP[7]. As in human ALCL and mouse models, the reduced or absent expression of WASP increases the abundance of active CDC42, we reasoned that lymphocytes from patients with absent or very low WASP expression should display higher CDC42 activation than control lymphocytes. We characterized EBV-immortalized B lymphocytes from three WAS patients with defined *WAS* mutations (Supplementary Fig. 9a) and low or absent WASP expression (Supplementary Fig. 9b). Indeed, lymphocytes from WAS patients showed higher levels of CDC42 activation than control cells (Supplementary Fig. 9c), in keeping with observations in NPM-ALK lymphoma cells. In addition, WAS lymphocytes showed decreased phosphorylation of STAT3 and AKT, consistent with defective cytokine production in WASP deficient lymphocytes[35], but showed higher levels of ERK and S6 phosphorylation, consistent with increased activation of the MAPK pathway (Supplementary Fig. 9b). These data show that lymphocytes from WAS patients with absent WASP expression have higher activity of CDC42 and MAPK signaling, suggesting the possibility that the predisposition of WAS patients to lymphoma could be associated to an intrinsic aberrant signaling in their lymphocytes.

DISCUSSION

WASP and WIP are essential regulators of the cytoskeleton in hematopoietic cells. Proper cytoskeletal regulation is fundamental for a variety of functions in lymphocytes and other hematopoietic cells, including lymphocyte proliferation and homeostasis[7]. WAS patients have a variable degree of immunodeficiency and an overall increased risk of developing hematologic malignancies, mostly lymphomas, that are thought to develop because of the immunodeficiency state[10]. In this work we provide evidence that WASP is an oncosuppressor in T lymphocytes and we identify ALCL as a specific subtype of T cell lymphoma where WASP and WIP expression is selectively down-regulated and contributes to lymphoma pathogenesis. An interesting expansion of this work would be to study WASP and WIP expression in B cell lymphoma or other hematologic malignancies. Furthermore, we provide evidence that the levels of the Rho GTPase CDC42 are essential for the tumor suppressor functions of WASP. The acceleration of lymphoma development in *Wasp*$^{-/-}$ mice

was dependent on the abundance of CDC42 in lymphoma cells; *Wasp*$^{-/-}$ lymphomas had significantly higher amount of active GTP-bound CDC42 and a reduction of about half CDC42 protein was sufficient to revert the phenotype *in vitro* and *in vivo* (Fig. 3d, Fig. 4b,c). Similar WASP-dependent regulation of active CDC42 was found in human ALCL (Fig. 6b) as well as in immortalized B lymphocytes from WAS patients (Supplementary Fig. 9c) demonstrating that active CDC42 accumulates in normal and tumor lymphocytes in the absence of WASP.

Due to the known role of WASP and WIP in T cell activation, we considered the possibility that the accelerated lymphoma development observed in WASP and WIP deficient mice could be associated to a defective immunosurveillance. However, several findings suggest that defective immunosurveillance is not sufficient to explain the accelerated lymphomagenesis in WASP and WIP deficient mice. First, in contrast to other classical immunodeficient strains such as NOD SCID mice, *Wasp*$^{-/-}$ and *Wip*$^{-/-}$ mice do not develop spontaneous lymphomas or other tumors[2,9], thus implying that the level of immunodeficiency is likely mild in these mice. Second, T cell functional defects are more pronounced in *Wip*$^{-/-}$ mice than in *Wasp*$^{-/-}$ mice[2], yet the acceleration of lymphomagenesis is comparable in the two genetic backgrounds. Third, *Wasp*$^{-/-}$*/Cdc42*$^{f/+}$*/CD4-Cre* T cells had defective T cell proliferation (Supplementary Fig. 10a) and defective MAPK pathway activation (Supplementary Fig. 10b) similar to *Wasp*$^{-/-}$ T cells, yet the loss of one copy of *Cdc42* is sufficient to revert the lymphoma acceleration observed in *Wasp*$^{-/-}$ mice (Fig. 3d). Fourth, if the immunodeficiency of *Wasp*$^{-/-}$ mice would be a major contribution to the accelerated lymphomagenesis, *Wasp*$^{-/-}$ lymphoma should have incurred into a limited immunoediting and have growth significantly impaired when transplanted into immunocompetent mice. In contrast, WT and *Wasp*$^{-/-}$ lymphoma grew equally in immunocompetent mice (Supplementary Fig. 10c). Finally, experiments in human ALCL clearly show that the cellular levels of WASP and WIP intrinsically contribute to lymphoma growth *in vitro* and *in vivo*.

We showed that WASP and WIP expression are selectively decreased in ALCL, a subtype of T cell lymphoma that can be driven by translocations involving the ALK gene in ALK-positive ALCL or by translocations involving other tyrosine kinases or phosphatases in ALK-negative ALCL[14,15]. Interestingly, aberrant STAT3 activation is frequent in both ALK + and ALK- ALCL where STAT3 phosphorylation is directly controlled by ALK or other oncogenic tyrosine kinases such as ROS1 and TYK2 in ALK- ALCL[14,36]. We showed that ALK oncogenic activity mediates down-regulation of WASP and WIP through a STAT3 and C/EBP-β dependent transcriptional repression. ChIP-seq experiments showed that abrogation of STAT3 activation by ALK inhibitors resulted in a profound genome-wide loss of STAT3 binding as well as at *WAS* and *WIPF1* genes (Fig. 5g–i and Supplementary Fig. 6b,c) Therefore, WASP and WIP down-regulation could represent a common feature of T cell lymphomas where the activity of STAT3 predominates, typically those induced by deregulated tyrosine kinases such as ALCL. In contrast, AITL and PTCL are more dependent on a tonic TCR signaling that relies on the maintenance of cytoskeletal signaling functions in which WASP and WIP are essential. However, TCR ligation induces WASP degradation that in turn modifies assembly of F-actin. Thus, reduced levels of WASP after TCR engagement could also play a role in downstream signaling in normal T cells[37].

Other mechanisms may contribute to the down-regulation of WASP or WIP in ALCL. For example, a recent study showed NPM-ALK directly phosphorylates Tyr102 of WASP; this phosphorylation impairs the binding of WASP to WIP and increases proteasome-dependent WASP degradation[38], overall confirming that ALK down-regulates WASP expression by multiple mechanisms. In contrast to our findings, however, this study concluded that WASP contributes to the oncogenic activity of ALK. This discrepancy likely originates from a different approach that focused on abrogating the residual WASP expression by shRNA rather than investigating the overall low levels of WASP in ALCL.

Whereas *WAS* and *WIPF1* mutations in ALCL have not been systematically studied, interestingly somatic loss of function (*WAS*^{G229E}) or frame-shift mutations (*WAS*^{G333fs} and *WAS*^{P329fs}) leading to premature WASP truncation similar to WAS patients have been detected in 4.6% of PTCL-NOS[19], raising the intriguing possibility that a fraction of other T cell lymphomas rely on somatic inactivation of WASP. In an ongoing effort to characterize *WAS* and *WIPF1* genes in ALCL, we performed whole-exome sequencing in 6 cases of ALK-positive ALCL. No somatic mutations of the *WAS*, *WIPF1 and CDC42* genes were found, but deletions of chromosome X in the region containing the *WAS* gene was detected in 2 out of 6 cases, suggesting that gene deletion could be an additional mechanisms for WASP inactivation in ALCL. Furthermore, we found one case with a mutation of the intersectin 2 (*ITSN2*) gene and two cases with mutations of the Myosin Heavy Chain 8 (*MYH8*) genes (Supplementary Table 1). ITSN2 is a GEF for CDC42 and regulates its activation[39] and interacts directly with WASP[40]. MYH8 is associated with the PAK and GTPase pathways. Interestingly this gene was recently found mutated also in ALK-negative ALCL[14]. These are limited observations that need to be expanded in larger series of cases but could underlie additional potential mechanisms that alter the CDC42/WASP axis in T cell lymphoma.

Taken together, it is tempting to propose that T cell lymphomas can be divided into two main categories. In T cell lymphomas that retain TCR signaling dependence, such as PTCL-NOS and AITL, WASP and WIP functions are maintained, at least initially, as they are key molecules for the immunological synapse and TCR signaling; once lymphoma is established, inactivating mutations of WASP could be further selected by providing additional growth advantage. On the other hand, in T cell lymphomas that lost TCR signaling and depend on aberrant tyrosine kinase activity, such as ALCL, WASP and WIP are lost or down-regulated as they act as tumor suppressor; their down-regulation provides a biological advantage by increased active CDC42 and MAPK signaling. In these lymphomas, the hyper-activated MAPK pathway could represent an actionable therapeutic vulnerability when combined with the inhibition of ALK, which is the driver oncogene in ALK+ ALCL. Thus, inhibition of both ALK and MEK inhibitor could represent a more powerful therapeutic strategy in ALK+ ALCL, possibly for those patients who respond poorly to crizotinib[33]. A similar concept has been recently suggested for ALK+ lung cancers[34].

In conclusion, by combining genetic and functional assays we have demonstrated an unexpected role for WASP and WIP as oncosuppressor proteins in lymphomas. Mechanistically, we have shown that the levels of CDC42 activation are increased in the absence of a binding to WASP, leading to increased proliferation and survival of lymphoma

cells. The activation of CDC42 and MAPK pathway provides a therapeutic vulnerability in lymphoma with low WASP expression.

METHODS

Transgenic mice and tumor xenograft

CD4-NPM-ALK transgenic mice [25], *CD4-Cre* [36], *Cdc42*$^{f/f}$ [41], *Wasp*$^{-/-}$ [9] and *Wip*$^{-/-}$ [2] were previously described. *CD4-NPM-ALK*, *Wasp*$^{-/-}$ and *Wip*$^{-/-}$ were bred in C57BL/6 background. NSG immunocompromised mice were purchased from Charles River Laboratories. For subcutaneous (s.c.) xenografts, human ALCL cell lines transduced with inducible lentiviral vectors expressing WASP and WIP cDNA were injected in both flanks of NSG mice. 5×10^6 of cells were resuspended in 150μL PBS and injected. Injected mice were administered drinking water containing doxycycline (1 mg/ml) (Sigma) in order to express WASP and WIP cDNA. Tumor growth was measured with a caliper every two days. Mice were sacrificed at humane endpoint and tumors were resected with a scalpel and snapped frozen or paraffin fixed in buffer neutral formalin for further experiments.

Mice were treated with trametinib (1.5 mg/Kg), or crizotinib (30 mg/Kg), or a combination of the two inhibitors, by oral gavage once a day for a week. Tumor growth was measured with a caliper every two days. Both drugs were dissolved in 0,5% methylcellulose + 0,05% Tween-80. Mice were sacrificed at humane endpoint.

Lymphoma cell lines obtained from *NPM-ALK* transgenic mice were injected s.c. in both flanks of syngeneic C57BL/6 or NSG mice. 10×10^6 cells were resuspended in 150μL PBS and injected. Tumor growth was followed as described above.

Mice were handled and treated in accordance with European Community guidelines under the mouse protocol approved by the Italian Ministry of Research (n. 254/2017-PR).

Cell Lines and Reagents

Human ALK+ ALCL cell lines (TS, SU-DHL1, JB6, Karpas-299, DEL, SUP-M2 and L82) and ALK- cell lines (MAC-1, FePD and Jurkat) ALCL cell lines were obtained from DSMZ (German collection of Microorganisms and Cell Cultures). Cell lines were maintained in RPMI 1640 (Lonza) with 10% fetal bovine serum (FBS), 2% penicillin, streptomycin 5 mg/ml, (Gibco) and 1% glutamine (Gibco). Cell lines were grown at 37°C in humidified atmosphere with 5% CO2. ALCL cell lines transduced with doxycicline-inducible shRNA to knock-down ALK expression were previously described [32].

HEK-293T and 293 Phoenix packaging cells were obtained from DSMZ and cultured in DMEM 10% FBS, 2% penicillin, streptomycin 5 mg/ml, and 1% glutamine.

ALK-positive Ki-JK and ALK negative T cell lymphoma lines were kindly provided by Dr. David Weinstock (Dana-Farber Cancer Insitute, Boston, USA). DL-40 (ALK-negative ALCL) were maintained in IMDM + 20% FBS; Ki-JK, OCI-Ly13.2 (T cell lymphoma) and OCI-Ly12 (PTCL-NOS) maintained in RPMI + 10% FBS, MAC2A (ALK-negative ALCL) maintained in RPMI + 20% FBS, DERL2 (hepatosplenic T cell lymphoma) maintained in

RPMI + 20% FBS + 100 U/ml human IL-2. ALK-positive COST cell line were kindly provided by Dr. Laurence Lamant (Centre de Recherche en Cancérologie de Toulouse, France).

Immortalized EBV-transformed B lymphoblastoid cell lines were obtained from healthy control and WAS patients (enrolled in clinical protocol 04–09-113R) as previously described[42] and cultured in RPMI 1640 medium (Thermo Fisher Scientific, USA) supplemented with 10% FBS, 2% penicillin, streptomycin 5 mg/ml, (Gibco) and 1% glutamine (Gibco).

Murine lymphoma cell lines were obtained from transgenic mice with corresponding genotype. Briefly, at the humane endpoint mice were sacrificed and tumoral thymuses were resected. Single cell suspensions were prepared from fresh tumoral thymuses with mechanical disgregation and isolated by using 40 μm nylon cell strainer (BD Biosystems). Cells were grown in RPMI and cultured at least 4 weeks before proceeding with further experiments.

Virus preparation and cell transduction

Lentiviruses were produced using the 3rd generation production system. Briefly, 293T cell lines were cultured in DMEM with 10% FBS. Cells at 70% confluency were co-transfected with pVSVG, pCMVR8.74, pRSV-Rev and a lentiviral vector expressing the construct of interest. Media was replenished 12/18h after transfection, and the supernatant was collected after 24 and 48h. Collected supernatants were filtered through 0.22 μm filter, concentrated by ultracentrifugation (50,000 X g for 2hr) and resuspended in 500 μl of sterile PBS. For infection, 5×10^4 cells were infected with the prepared lentivirus along with polybrene (8μg/ml), cells with viral particles were spun down at 2500 RPM for 90 minutes and then incubated at 37° overnight.

STAT3- and *C/EBP-β*-specific shRNAs and inducible *ALK* shRNA have been previously described [43,44]. Human Flag-WASP and Flag-WIP cDNA were obtained from Dr. A. Galy (Institut Gustave Roussy, Villejuif, France) and from Addgene, respectively. For the doxycycline inducible system (Tet-ON), WASP and WIP cDNA were cloned into modified pCCL vector as previously described [45]. SU-DHL1, JB6, DEL and Karpas-299 cell lines were co-infected with pCCL and rtTA plasmids. For cell sorting enrichment, cells were induced with 1ug/ml doxycycline for 12h and sorted for GFP expression on a MoFlo High-Performance Cell Sorter (DAKO Cytomation).

Retroviruses were generated by transfection of pWZL Blast vector expressing CRE-ERT2 in 293 Phoenix packaging cells. Transfected cells were incubated at 37° C for 12/18h and supernatants containing viral particles were collected at 24 and 48 hours. 300 μl retroviral supernatants were used to transduce 5×10^4 lymphoma cells as previously described [23]. CRE-ERT2 transduced cells were selected using blasticidin (Calbiochem) at 25 μg/ml for 6 days.

Cell Lysis and Immunoblotting

Total cellular protein were extracted with GST-FISH buffer (10mM MgCl2, 150mM NaCl, 1% NP40, 2% Glycerol, 1mM EDTA, 25mM HEPES pH 7.5), added with 1 mM

phenylmethylsulfonyl fluoride (PMSF), 10 mM NaF, 1 mM Na3VO4, and protease inhibitors (Roche, Mannheim, Germany). Total cell lysate were cleared by centrifugation (13,000 rpm) at 4° C in a microcentrifuge for 10 min and quantified using the Bio-Rad protein assay method. Protein samples were normalized based on protein concentration, denaturated by addition of Laemmli buffer and boiled for 10 min. Thirty to fifty micrograms of proteins were run on sodium dodecyl sulfate–polyacrylamide gel electrophoresis (SDS-PAGE) under reducing conditions and transferred to nitrocellulose (GE Healthcare). Membranes were incubated with specific antibodies, detected with peroxidase-conjugated secondary antibodies (GE Healthcare) and enhanced using chemiluminescent reagent (Amersham). The following primary antibodies were used: anti-ALK (Invitrogen, Catalog#: 35–4300), anti-human WASP (Epitomics, Clone:EP2541Y, Catalog#:2422–1), anti-murine WASP (Cell Signaling Technology, Catalog#:4860), anti-N-WASP (Cell Signaling Technology, Clone:30D10, Catalog#:4848), anti-WIP (Santa Cruz Biotechnology, Clone:H-224, Catalog#:sc-25533), anti-phospho-STAT3 (Tyr705) (Cell Signaling Technology, Catalog#:9131), anti-STAT3 (Cell Signaling Technology, Clone:79D7, Catalog#:4904), anti-phospho-ERK (Thr202/Tyr204) (Cell Signaling Technology, Catalog#: 9101), anti-ERK (Cell Signaling Technology, Catalog#:9102), anti-phospho-AKT (Ser473) (Cell Signaling Technology, Clone:D9E, Catalog#:4060), anti-AKT (Cell Signaling Technology, Clone:11E7, Catalog#:4685), anti-phospho-JNK (Thr183/Tyr185) (Cell Signaling Technology, Catalog#:9255), anti-JNK (Cell Signaling Technology, Catalog#: 9252), anti-CDC42 (BD Transduction Laboratory, Catalog#:610929), anti-C/EBPβ (Santa Cruz Biotechnology, Clone:C-19, Catalog#:sc-150), anti-Cleaved Caspase-3 (Asp175) (Cell Signaling Technology, Catalog#:9661), anti-phospho S6 (Cell Signaling Technology, clone D57.2.2E, Catalog#:4858) and anti-S6 (Cell Signaling Technology, clone 54D2, Catalog#: 2317), HSP90 (Santa Cruz Biotechnology, #H114), anti-ZAP70 (Millipore, Clone:2F3.2, Catalog#:05–253) anti-GFP (Invitrogen, Catalog #:A-11122), anti-Actin (Sigma-Aldrich, Catalog#:A2066).

Histology, immunohistochemistry and Immunofluorescence

For histology, tissue samples were formalin fixed and paraffin embedded, cut into 4 μm thick sections and stained with hematoxylin and eosin.

For immunohistochemistry, formalin-fixed sections were de-waxed in xylene, dehydrated by passage through graded alcohols to water; sections were microwaved in citrate buffer pH 6 for 15 minutes and then transferred to PBS. Endogenous peroxidase was blocked using 1.6% hydrogen peroxide in PBS for 10 minutes followed by washing in distilled water. Normal serum diluted to 10% in 1% BSA was used to block non-specific staining.

The slides were than incubated for 1 hour with the following primary antibodies: anti-WASP (Epitomics), anti-WIP (clone H-224, Santa Cruz Biotechnology), anti-ALK (clone: 18–0266, Zymed); anti-Cleaved Caspase-3 (Cell Signaling Technology), anti-murine Ki-67 (AbCam, Clone: SP6, Catalog#:ab16667) and anti-human Ki-67 (DAKO, Clone: MIB-1, Catalog#:M7240). After washing, sections were incubated with biotinylated secondary goat antibody to rabbit IgG and visualized with the EnVision system (Dako).

For immunofluorescence, cells were plated on glass coverslips pretreated with fibronectine (10 μg/mL PBS) at 37°C for 1 hour and incubated overnight in fresh medium. Samples were fixed in 4% paraformaldehyde at room temperature for 10 minutes and permeabilized with 0.3% Triton X-100 for 5 minutes. Coverslips were incubated with 3% bovine serum albumin (BSA) for 1 hour at room temperature and then stained with phycoerythrin (PE)–conjugated phalloidin (1:500, Sigma) and HOECHST (300 ng/mL, Sigma). Coverslips were mounted on microscope slides using anti-fading solution and viewed using a Leica photomicroscope. Images were acquired at room temperature by means of HCX PL APO 100x /1.40 OIL (Leica, Heidelberg, Germany) and analysed by DM LM Leica software. Cell dimension has been measured using ImageJ software.

The slides were reviewed by experience hematopathologists and quantification of the levels of WASP and WIP expression was performed selectively in multiple areas where lymphoma cells were clearly enriched. This selection was achieved by comparing the areas on serial sections stained with the following markers: ALK for ALK+ ALCL, CD30 for ALK- ALCL, CD10 for AITL. When a marker was not available (such as loss of a particular T cell antigen) for PTCL-NOS, NK/T cell lymphoma and hepatosplenic γδ T cell lymphoma, the selection of the areas with enriched lymphoma cells was based on morphologic criteria, such as cluster of atypical cells or invasion of specific structures such as vessels in NK/T cell lymphoma or sinusoids in hepatosplenic γδ T cell lymphoma. The quantification of WASP and WIP expression levels was achieved by comparison with an internal control constituted by normal B and T lymphocytes.

Quantitative Real-Time (qRT) PCR analysis

Total RNA was extracted from cells using TRIZOL solution (Invitrogen), followed by cDNA preparation from 1 μg of total RNA. cDNA products were quantified by real-time PCR using SYBR Green Supermix (Biorad) on Bio-Rad iCycler iQ Real-Time PCR Detection System. Normalization was performed against the housekeeping human acidic ribosomal protein (*HuPO*) or Actin according to the formula $2^{-\Delta\Delta Ct}$, where the ΔC_t=¼ Ct (threshold cycle) gene of interest -C_t internal control, as indicated by the manufacturer.

WASP-specific primers: forward 5′-GAAACGCTCAGGGAAGAAGA-3′, reverse 5′-CTGCCCTGGAGAAACGACTC-3′;

WIP-specific primers: forward 5′- ACAGGGATAATGATTCTGGAGG −3′, reverse 5′-CTGGAGAAGGCACAGGAAAC −3′

HuPO-specific primers: forward5’-GCTTCCTGGAGGGTGTCC-3’, reverse 5’-GCTTCCTGGAGGGTGTCC-3’

ACTIN-specific primers: forward 5’- ACCGAGGCCCCCCTGAAC −3’, reverse 5’-CAGGTCCAGACGCAGGATGGC-3’

LAT-specific primers forward 5′-ACAGTGTGGCGAGCTACG-3’, reverse 5′-CGTTCACGTAATCATCAATGG-3’

DNA demethylation

ALK+ ALCL cell lines (TS, SU-DHL1 and JB6) were plated in 6-well plate (5×10^5 cells/mL), treated with 5 μM of the methyltransferase inhibitor 5-aza-2-deoxycytidine (Sigma). Cells were washed twice in PBS and collected at 0, 48, 72, 96, 144 hours after the treatment. Cells were collected for Western Blot and qRT PCR assays.

ZAP 70 and LAT were used as positive controls for western blot and qRT PCR, respectively as previously reported [30].

Chromatin Immunoprecipitation (ChIP)

JB6 and SU-DHL1 cells were fixed in 1% formaldehyde (Sigma Aldrich, F8775) for 10min at 37°C. Subsequently, glycine was added to 125mM and incubated at 37°C for 5min at 37°C. Next, cells were pelleted and washed twice with cold PBS. Pellets were stored at −80°C until use.

Nuclei from 10M cells per ChIP-seq were extracted, and chromatin was sonicated with a Covaris sonicator. Immunoprecipitation reactions were performed overnight with anti-STAT3 (Cell Signaling Technology, Clone:124H6, Catalog#:9139) or anti-C/EBP-β (Abcam, Clone:E299, Catalog#:ab32358) antibodies. The next morning, antibodies and chromatin were captured using Protein G Dynabeads (Thermo Fisher). Material was washed, eluted, and treated with RNAse A (Roche 11 119 915 011) for 30min at 37°C and Proteinase K (Life Technologies 100005393) for 3 hours at 65°C. DNA was extracted using SPRI beads (Beckman Coulter Agencourt AMP Xpure).

H3K4me3, H3K27ac and H3K27me3 profiles on Jurkat[46–48] and GM12878[49] cell lines were obtained from public databases including ENCODE.

Library Preparation and Sequencing—Library preparation of ChIP-seq DNA was performed using the Ultra II Library Prep Kit (NEB E7103L) and Multiplex Oligos for Illumina (NEB E7335L) and sequenced on an Illuminia Nextseq 500 (75bp single end).

ChIP-seq Data Processing.—ChIP-seq samples were sequenced with the Illumina NextSeq technology, and output data were demultiplexed and converted to FASTQ format using the bcl2fastq software tool. Read quality was assessed by FASTQC, and ChIP-seq reads were aligned to the hg19 genome with Bowtie2 v2.29 in the -k 1 reporting mode[50]. Output BAM files were converted into BigWig track files using the “callpeak” function of MACS2 v2.1.1 with the “-B --SPMR” option followed by the use of the BEDTools [51] “sort” function and the UCSC utility “bedgraphToBigWig” [52], and the tracks were visualized in IGV v2.4.3. Narrow peaks were called with the MACS2 v2.1.1 software using input as controls and a q-value cutoff of 0.001[53]. Metaplots and heat maps were generated using ngsplot v2.61[54].

Gene expression profiling

Total RNA was extracted from primary *NPM-ALK/Wasp*$^{+/+}$ or *NPM-ALK/Wasp*$^{-/-}$ lymphoma using TRIZOL reagent (Invitrogen) and purified using the RNeasy total RNA

Isolation Kit (Qiagen). GeneChip Mouse Gene 1.0 ST Array from Affymetry was used for profiling.

Apoptosis assay and cell cycle analysis

Cre-ERT2 transduced murine cells were grown in 6-well plates after treatment with 10nM 4-hydroxytamoxifen (4-OHT; Sigma) for 4 hours. At 0, 24 and 48 hours after the treatment cells were stained with 200nM tetrametylrodamine methyl-ester (TMRM) for 15 minutes in dark, washed twice in PBS and the percentage of apoptotic cells were measured by flow cytometry (BD FACSCALIBUR) using CellQuest Program.

For cell cycle analysis the DNA content was determinated with propidium iodide staining. SU-DHL1 and Karpas-299 cell lines either expressing WASP and WIP inducible vector or the GFP control were treated for 168 hours with doxycycline (1ug/ml), cells were washed with PBS, resuspended in citric acid buffer (0.05 M Na2HPO4, 25 mM sodium citrate, and 0.1% Triton X-100 [pH 7.3]), treated with RNase (0.25 mg/mL), and then stained with propidium iodide (50 μg/mL) 15 minutes at 37ºC in the dark. The G_1 and S/G_2-M cell fractions were calculated for the non-apoptotic cell population only.

Cell viability assay

Cell viability assay on human ALK+ ALCL cell lines was performed using CellTiter-Glo (Promega) according to manufacturer's instruction. Briefly, cells were seeded into white walled 96-well plates (3 wells/sample) in presence/absence of treatment (doxycycline, 4-hydroxytamoxifen or trametinib). CellTiter-Glo reagent was added to each well and luminescence output data were taken at 0, 24, 48 and 72 hours by GloMax-Multi Detection System (Promega). Trametinib was purchased from Selleckem, diluted in DMSO and used at the indicated concentrations.

Drug sensitivity assay

Drug sensitivity assays have been performed as previously described[55], Briefly, cells (2×10^3) were seeded in 96-well plates in RPMI complete medium. The following day, cells were treated with selumetinib (Selleckchem, Cat# S1008), trametinib (Selleckchem Cat# S2673), crizotinib (kindly provided by Pfizer), MEK162 (Selleckchem Cat# S7007) or PD0325901 (Selleckchem Cat# S1036) using a ten-point dose titration scheme from 1nM to 10μM or from 1nM to 1μM. After 72 hours, cell viability was assessed using colorimetric MTS assay (CellTiter 96® AQueous Non-Radioactive Cell Proliferation Assay (MTS) Powder, Promega). Absolute inhibitory concentration (IC) values were calculated using four-parameter logistic curve fitting. All experimental points were a result of three to six replicates, and all experiments were repeated at least three times. The data was graphically displayed using GraphPad Prism 7 for Windows (GraphPad Software). Each point (mean ± standard deviation) represents growth of treated cells compared to untreated cells. The curves were fitted using a non-linear regression model with a sigmoidal dose response.

Measurement of GTP-bound CDC42

To measure the amount of GTP-bound CDC42 cells were plated at the same concentration in 6-well plates and incubated in RPMI medium overnight. Cells were collected and lysed as

previously described. CDC42 activity was determined using CDC42 G-LISA™ assay kit in accordance with the manufacturer's instructions (Cytoskeleton Inc.). Briefly, cells were collected, washed three times in ice cold PBS on cold centrifuge, protein lysates were transferred to ice-cold 1.5-ml centrifuge tubes and clarified by centrifuging at 10,000 rpm for 2 min and immediately snapped frozen in liquid nitrogen. Protein concentrations were determined using the Precision Red Advance Protein Assay (Cytoskeleton), and 1.0 mg/ml protein was used for the GTPase activation assay. 50 μl of protein lysate were added to pre-coated 96-well plate, the plate was washed, and antigen-presenting buffer was added, followed by primary and secondary antibodies. The reaction was detected using horseradish peroxidase detection reagent followed by the stop buffer. The plate was read immediately by measuring absorbance at 490 nm on a microplate spectrophotometer.

Human ALCL cell lines, stably transfected with Tet-ON WASP & WIP, and the empty control Tet-ON GFP plasmid, were treated with doxycycline (1μg/mL). After 48 hours cells were lysed and GTP-bound CDC42 was immunoprecipitated using CDC42 Activation Assay Kit (NewEast Biosciences). Quantification was performed by densitometric analysis of the Western blot bands.

Flow cytometry

Six-weeks old mice were sacrificed and thymuses were resected and used for flow cytometry analysis. Single cell suspensions were prepared from fresh pre-tumoral thymuses with mechanic disgregation and isolated by using 40 μm nylon cell strainers (BD Biosystems, San Jose, CA, USA). Cells were resuspended in PBS and stained with the following antibodies: PE-anti-mouse CD4 (clone GK1.5; Miltenyi Biotec), and PerCP-anti-mouse CD8a (clone 53–6.7; BioLegend) for 15 minutes, then washed and resuspended in PBS. Cells were then acquired in a FACSCalibur flow cytometer (BD Bioscience) and analysed using the FlowJo software.

For co-colture assays, SU-DHL1 and JB6 cell lines either expressing WASP and WIP inducible vector or the GFP control were mixed 1:1 with parental cells, the percentage of GFP positive cells was followed over time for 40 days by flow cytometry.

T-cell purification, *ex vivo* activation and proliferation analysis

Untouched T cells were isolated from spleens of WASP- and WIP- deficient mice and wild-type mice by immunomagnetic depletion of B cells, monocytes/macrophages, NK cells, dendritic cells, erythrocytes, and granulocytes.

Briefly, spleens were collected, placed on ice, washed in PBS to remove residual blood, cut into small pieces, crushed and physically dissociated using a Falcon cell strainer, and subjected to hypotonic lysis of erythrocytes. Cells were resuspended in isolation buffer (PBS supplemented with 0.1% BSA and 2mM EDTA). All non-T cells were depleted with a mixture of rat monoclonal IgG antibodies against non-T cells ("Antibody mix": anti mouse CD45R, CD11b, Ter-119, and CD16/CD32; Invitrogen) combined with Mouse Depletion Dynabeads (4.5 um diameter beads coated with a polyclonal sheep anti-rat IgG antibody; Invitrogen) following the manufacturer's instructions.

Isolated mouse T cells, bead- and antibody-free, were activated by adding Dynabeads Mouse T-Activator CD3/CD28 (polyclonal activation; Invitrogen).

For T cell proliferation analysis purified and activated T cells (1×10^6 cells) were plated in 6-well plate and cultured at 37°C in RPMI 1640 medium supplemented with 15% FBS, 2% penicillin, streptomycin 5mg/ml and 50 mM 2-mercaptoethanol for 48 hours. Cells were then collected for CellTiter-Glo analysis (Promega) following the manufacturer's instructions.

For Western Blot analysis cells were collected after 15 minutes of incubation with the cocktail of CD3/CD28 beads, centrifuged and washed with cold PBS for protein extraction.

Statistical analysis

Statistical analysis was performed with GraphPad PRISM 7.0 software. *P* values were calculated by using the unpaired, two-tailed Student's t-test with Welch's correction as indicated in each figure legend. Kaplan-Meier analysis for survival curve was performed with GraphPad Prism 7 and *P* values were determined with a log-rank (Mantel-Cox) test.

Supplementary Material

Refer to Web version on PubMed Central for supplementary material.

ACKNOWLEDGEMENTS

We would like to thank Maria Stella Scalzo and Daniele Corino for technical assistance, Barbara Castella for providing purified human T cells. The work has been supported by grants FP7 ERC-2009-StG (Proposal No. 242965 - "Lunely")(R.C.), R01 CA196703–01 (R.C.); AIRC grant MFAG (C.A. and M.C.); National Research Foundation of Korea (NRF) fellowship 2016R1A6A3A03006840 (T-C.C.); Bando Giovani Ricercatori 2009-GR 1603126 (M.C.); MINECO/FEDER SAF2015–70368-R and Fundación Ramón Areces (I.M.A.); the Division of Intramural Research, National Institute of Allergy and Infectious Diseases, NIH (L.D.N.); Award T32GM007753 from the National Institute of General Medical Sciences (S.H.C.) (the content is solely the responsibility of the authors and does not necessarily represent the official views of the National Institute of General Medical Sciences or the National Institutes of Health); in part by awards from the NIH DP2 New Innovator Award 1DP2CA195762–01(C.K.); the American Cancer Society Research Scholar Award RSG-14–051-01-DMC and the Pew-Stewart Scholars in Cancer Research Grant (C.K.).; the European Union Horizon 2020 Marie Sklodowska-Curie Innovative Training Network (ITN-ETN) Grant, Award No.: 675712 for the European Research Initiative for ALK-Related Malignancies (ERIA) (G.G.S., I.M., C.GP., R.C.).

REFERENCES

1. Sullivan KE, Mullen CA, Blaese RM & Winkelstein JA A multiinstitutional survey of the Wiskott-Aldrich syndrome. J Pediatr 125, 876–885 (1994). [PubMed: 7996359]
2. Anton IM, et al. WIP deficiency reveals a differential role for WIP and the actin cytoskeleton in T and B cell activation. Immunity 16, 193–204 (2002). [PubMed: 11869681]
3. de la Fuente MA, et al. WIP is a chaperone for Wiskott-Aldrich syndrome protein (WASP). Proceedings of the National Academy of Sciences of the United States of America 104, 926–931 (2007). [PubMed: 17213309]
4. Ramesh N & Geha R Recent advances in the biology of WASP and WIP. Immunol Res 44, 99–111 (2009). [PubMed: 19018480]
5. Ramesh N, Anton IM, Hartwig JH & Geha RS WIP, a protein associated with wiskott-aldrich syndrome protein, induces actin polymerization and redistribution in lymphoid cells. Proceedings of the National Academy of Sciences of the United States of America 94, 14671–14676 (1997). [PubMed: 9405671]

6. Abdul-Manan N, et al. Structure of Cdc42 in complex with the GTPase-binding domain of the 'Wiskott-Aldrich syndrome' protein. Nature 399, 379–383 (1999). [PubMed: 10360578]
7. Thrasher AJ & Burns SO WASP: a key immunological multitasker. Nature reviews. Immunology 10, 182–192 (2010).
8. Massaad MJ, Ramesh N & Geha RS Wiskott-Aldrich syndrome: a comprehensive review. Ann N Y Acad Sci 1285, 26–43 (2013). [PubMed: 23527602]
9. Snapper SB, et al. Wiskott-Aldrich syndrome protein-deficient mice reveal a role for WASP in T but not B cell activation. Immunity 9, 81–91 (1998). [PubMed: 9697838]
10. Ochs HD & Thrasher AJ The Wiskott-Aldrich syndrome. The Journal of allergy and clinical immunology 117, 725–738; quiz 739 (2006). [PubMed: 16630926]
11. Recher M, et al. B cell-intrinsic deficiency of the Wiskott-Aldrich syndrome protein (WASp) causes severe abnormalities of the peripheral B-cell compartment in mice. Blood 119, 2819–2828 (2012). [PubMed: 22302739]
12. Boddicker RL, Razidlo GL & Feldman AL Genetic alterations affecting GTPases and T-cell receptor signaling in peripheral T-cell lymphomas. Small GTPases, 1–7 (2016).
13. Scarfo I, et al. Identification of a new subclass of ALK-negative ALCL expressing aberrant levels of ERBB4 transcripts. Blood 127, 221–232 (2016). [PubMed: 26463425]
14. Crescenzo R, et al. Convergent mutations and kinase fusions lead to oncogenic STAT3 activation in anaplastic large cell lymphoma. Cancer cell 27, 516–532 (2015). [PubMed: 25873174]
15. Parrilla Castellar ER, et al. ALK-negative anaplastic large cell lymphoma is a genetically heterogeneous disease with widely disparate clinical outcomes. Blood 124, 1473–1480 (2014). [PubMed: 24894770]
16. Werner MT, Zhao C, Zhang Q & Wasik MA Nucleophosmin-anaplastic lymphoma kinase: the ultimate oncogene and therapeutic target. Blood 129, 823–831 (2017). [PubMed: 27879258]
17. Yoo HY, et al. A recurrent inactivating mutation in RHOA GTPase in angioimmunoblastic T cell lymphoma. Nature genetics 46, 371–375 (2014). [PubMed: 24584070]
18. Sakata-Yanagimoto M, et al. Somatic RHOA mutation in angioimmunoblastic T cell lymphoma. Nature genetics 46, 171–175 (2014). [PubMed: 24413737]
19. Palomero T, et al. Recurrent mutations in epigenetic regulators, RHOA and FYN kinase in peripheral T cell lymphomas. Nature genetics 46, 166–170 (2014). [PubMed: 24413734]
20. Abate F, et al. Activating mutations and translocations in the guanine exchange factor VAV1 in peripheral T-cell lymphomas. Proceedings of the National Academy of Sciences of the United States of America 114, 764–769 (2017). [PubMed: 28062691]
21. Ambrogio C, et al. The anaplastic lymphoma kinase controls cell shape and growth of anaplastic large cell lymphoma through Cdc42 activation. Cancer research 68, 8899–8907 (2008). [PubMed: 18974134]
22. Colomba A, et al. Activation of Rac1 and the exchange factor Vav3 are involved in NPM-ALK signaling in anaplastic large cell lymphomas. Oncogene 27, 2728–2736 (2008). [PubMed: 17998938]
23. Choudhari R, et al. Redundant and nonredundant roles for Cdc42 and Rac1 in lymphomas developed in NPM-ALK transgenic mice. Blood 127, 1297–1306 (2016). [PubMed: 26747246]
24. Swerdlow SH, et al. The 2016 revision of the World Health Organization classification of lymphoid neoplasms. Blood 127, 2375–2390 (2016). [PubMed: 26980727]
25. Chiarle R, et al. NPM-ALK transgenic mice spontaneously develop T-cell lymphomas and plasma cell tumors. Blood 101, 1919–1927 (2003). [PubMed: 12424201]
26. Lanzi G, et al. A novel primary human immunodeficiency due to deficiency in the WASP-interacting protein WIP. The Journal of experimental medicine 209, 29–34 (2012). [PubMed: 22231303]
27. Al-Mousa H, et al. Hematopoietic stem cell transplantation corrects WIP deficiency. The Journal of allergy and clinical immunology 139, 1039–1040 e1034 (2017). [PubMed: 27742395]
28. Notarangelo LD, Notarangelo LD & Ochs HD WASP and the phenotypic range associated with deficiency. Curr Opin Allergy Clin Immunol 5, 485–490 (2005). [PubMed: 16264326]

29. Hill CS, Wynne J & Treisman R The Rho family GTPases RhoA, Rac1, and CDC42Hs regulate transcriptional activation by SRF. Cell 81, 1159–1170 (1995). [PubMed: 7600583]
30. Ambrogio C, et al. NPM-ALK oncogenic tyrosine kinase controls T-cell identity by transcriptional regulation and epigenetic silencing in lymphoma cells. Cancer research 69, 8611–8619 (2009). [PubMed: 19887607]
31. Hassler MR, et al. Insights into the Pathogenesis of Anaplastic Large-Cell Lymphoma through Genome-wide DNA Methylation Profiling. Cell reports 17, 596–608 (2016). [PubMed: 27705804]
32. Piva R, et al. Ablation of oncogenic ALK is a viable therapeutic approach for anaplastic large-cell lymphomas. Blood 107, 689–697 (2006). [PubMed: 16189272]
33. Gambacorti Passerini C, et al. Crizotinib in advanced, chemoresistant anaplastic lymphoma kinase-positive lymphoma patients. Journal of the National Cancer Institute 106, djt378 (2014).
34. Hrustanovic G, et al. RAS-MAPK dependence underlies a rational polytherapy strategy in EML4-ALK-positive lung cancer. Nature medicine 21, 1038–1047 (2015).
35. Rivers E & Thrasher AJ Wiskott-Aldrich syndrome protein: emerging mechanisms in immunity. European journal of immunology (2017).
36. Chiarle R, et al. Stat3 is required for ALK-mediated lymphomagenesis and provides a possible therapeutic target. Nature medicine 11, 623–629 (2005).
37. Watanabe Y, et al. T-cell receptor ligation causes Wiskott-Aldrich syndrome protein degradation and F-actin assembly downregulation. The Journal of allergy and clinical immunology 132, 648–655 e641 (2013). [PubMed: 23684068]
38. Murga-Zamalloa CA, et al. NPM-ALK phosphorylates WASp Y102 and contributes to oncogenesis of anaplastic large cell lymphoma. Oncogene 36, 2085–2094 (2017). [PubMed: 27694894]
39. Zhang J, et al. Intersectin 2 controls actin cap formation and meiotic division in mouse oocytes through the Cdc42 pathway. FASEB journal : official publication of the Federation of American Societies for Experimental Biology 31, 4277–4285 (2017). [PubMed: 28626024]
40. McGavin MK, et al. The intersectin 2 adaptor links Wiskott Aldrich Syndrome protein (WASp)-mediated actin polymerization to T cell antigen receptor endocytosis. The Journal of experimental medicine 194, 1777–1787 (2001). [PubMed: 11748279]
41. Wu X, et al. Cdc42 controls progenitor cell differentiation and beta-catenin turnover in skin. Genes & development 20, 571–585 (2006). [PubMed: 16510873]
42. Facchetti F, et al. Defective actin polymerization in EBV-transformed B-cell lines from patients with the Wiskott-Aldrich syndrome. J Pathol 185, 99–107 (1998). [PubMed: 9713366]
43. Martinengo C, et al. ALK-dependent control of hypoxia inducible factors mediates tumor growth and metastasis. Cancer research (2014).
44. Piva R, et al. Functional validation of the anaplastic lymphoma kinase signature identifies CEBPB and BCL2A1 as critical target genes. The Journal of clinical investigation 116, 3171–3182 (2006). [PubMed: 17111047]
45. Ceccon M, et al. Excess of NPM-ALK oncogenic signaling promotes cellular apoptosis and drug dependency. Oncogene 35, 3854–3865 (2016). [PubMed: 26657151]
46. Orlando DA, et al. Quantitative ChIP-Seq normalization reveals global modulation of the epigenome. Cell reports 9, 1163–1170 (2014). [PubMed: 25437568]
47. Mansour MR, et al. Oncogene regulation. An oncogenic super-enhancer formed through somatic mutation of a noncoding intergenic element. Science 346, 1373–1377 (2014). [PubMed: 25394790]
48. Manser M, et al. ELF-MF exposure affects the robustness of epigenetic programming during granulopoiesis. Sci Rep 7, 43345 (2017). [PubMed: 28266526]
49. Thurman RE, et al. The accessible chromatin landscape of the human genome. Nature 489, 75–82 (2012). [PubMed: 22955617]
50. Langmead B & Salzberg SL Fast gapped-read alignment with Bowtie 2. Nature methods 9, 357–359 (2012). [PubMed: 22388286]
51. Quinlan AR & Hall IM BEDTools: a flexible suite of utilities for comparing genomic features. Bioinformatics 26, 841–842 (2010). [PubMed: 20110278]

52. Kuhn RM, Haussler D & Kent WJ The UCSC genome browser and associated tools. Briefings in bioinformatics 14, 144–161 (2013). [PubMed: 22908213]

53. Zhang Y, et al. Model-based analysis of ChIP-Seq (MACS). Genome biology 9, R137 (2008). [PubMed: 18798982]

54. Shen L, Shao N, Liu X & Nestler E ngs.plot: Quick mining and visualization of next-generation sequencing data by integrating genomic databases. BMC Genomics 15, 284 (2014). [PubMed: 24735413]

55. Ambrogio C, et al. KRAS Dimerization Impacts MEK Inhibitor Sensitivity and Oncogenic Activity of Mutant KRAS. Cell 172, 857–868 e815 (2018). [PubMed: 29336889]

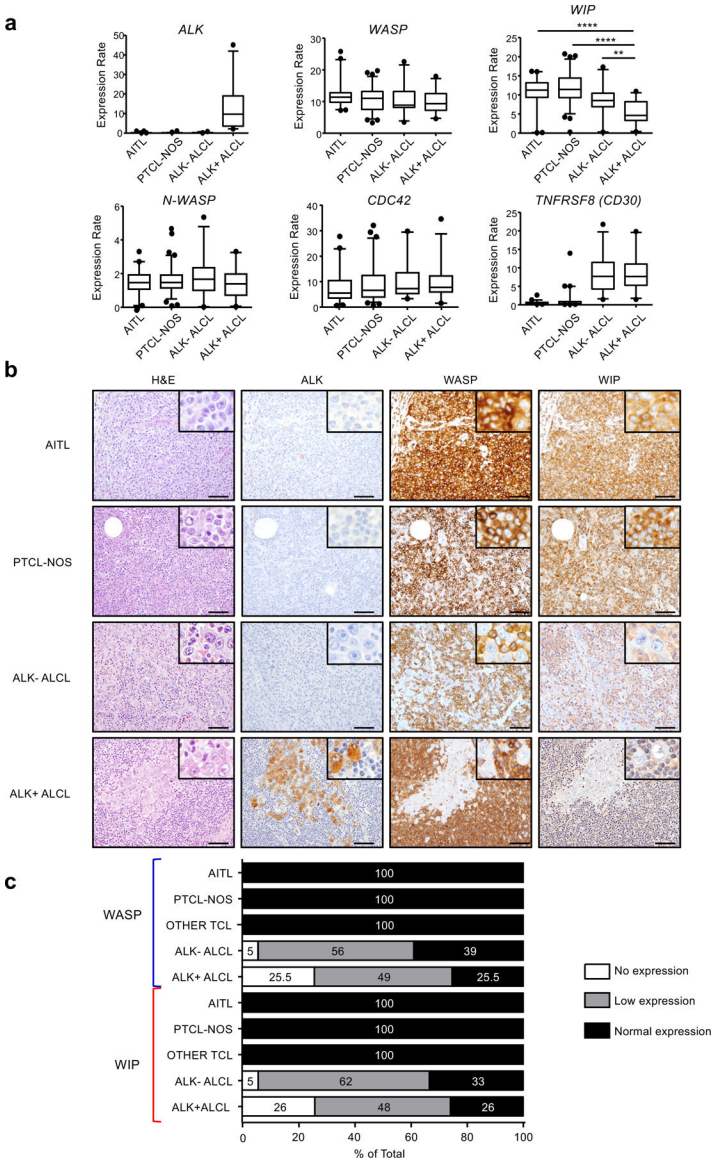

Figure 1. WASP and WIP are selectively down-regulated in Anaplastic Large Cell Lymphoma (ALCL)

(**a**) Gene-expression profiling analysis of *ALK, WASP, WIP, N-WASP, CDC42* and *TNFRS8 (CD30)* on different cases of human T cell lymphomas: AITL, n = 40; PTCL-NOS, n = 74; ALK- ALCL, n = 24, ALK+ ALCL, n = 30. The boxes represent the first and third quartiles, and the line represents the median. The whiskers represent the upper and lower limits of the range (ALK+ ALCL *vs* AITL, ****$P = 5.85 \text{ X } 10^{-6}$; ALK+ ALCL *vs* PTCL-NOS, ****$P = 6.08 \text{ X } 10^{-12}$; ALK+ ALCL *vs* ALK- ALCL, **$P = 0.0075$; significance was determined by unpaired, two-tailed Student's t-test). *TNFRS8 (CD30)* is strongly expressed in ALK- or ALK+ ALCL but not in other T cell lymphoma (TCL) subtypes.

(**b**) Representative hematoxylin and eosin staining and immunohistochemistry stainings performed with the indicated antibody on human T cell lymphoma subtypes. The number of human T cell lymphoma samples analysed is reported in Figure 1c. WASP antibody was validated in formalin fixed samples on samples with inducible WASP expression

(Supplementary Fig. 7f). WIP antibody cross reacts with mouse WIP and was validated on WIP knock-out cells (Supplementary Fig. 1b). Scale bar = 100μm. Insets: high magnification images.

(**c**) WASP and WIP expression in human T cell lymphoma subtypes. AITL, n = 20; PTCL-NOS, n = 20; ALK- ALCL, n = 29; ALK+ ALCL, n = 43 for WASP and n = 31 for WIP; other TCL are NK/T cell lymphoma, nasal-type, n = 3 and hepatosplenic γδ T cell lymphoma, n = 3. The number of patient samples is indicated for each lymphoma subtype. WASP and WIP expressions were quantified by immunostaining. Normal expression = expression equal to surrounding reactive T cells; Low expression = decreased expression compared to surrounding reactive T cells; No expression = absence of expression in lymphoma cells.

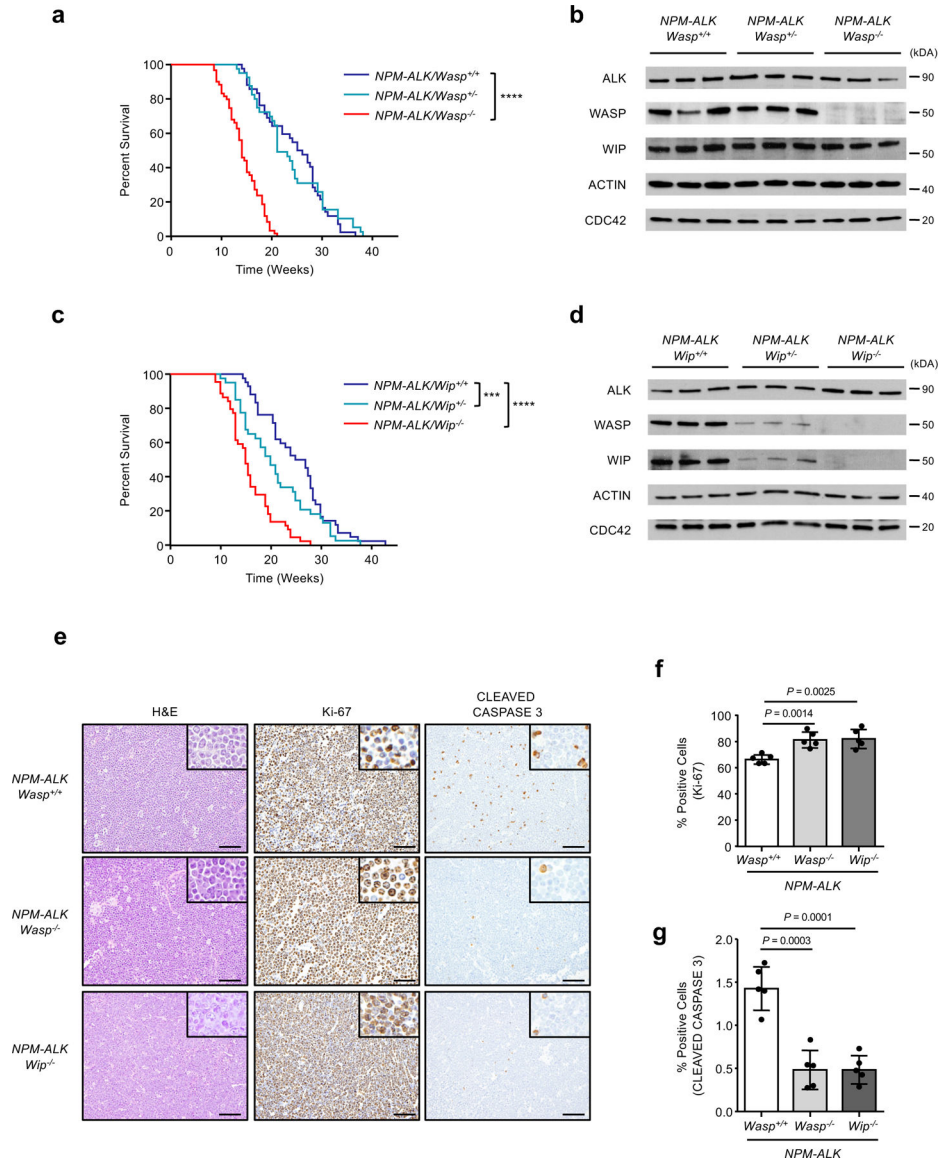

Figure 2. WASP is an oncosuppressor in ALK+ T cell lymphoma.

(**a**) Kaplan-Meier analysis of overall survival of NPM-ALK transgenic mice crossed with WASP deficient mice (Blue, *NPM-ALK/Wasp*$^{+/+}$, n= 35; Light blue, *NPM-ALK/Wasp*$^{+/-}$, n = 37; Red, *NPM-ALK/Wasp*$^{-/-}$, n= 30). The number of mice for each genotype is indicated. *NPM-ALK/Wasp*$^{+/+}$ *vs NPM-ALK/Wasp*$^{-/-}$, ****$P < 0.0001$; significance was determined by log-rank (Mantel–Cox) test.

(**b**) Western Blot analysis from n = 3 independent primary lymphomas isolated from *NPM-ALK* transgenic mice crossed with WASP deficient mice. The blot is representative of at least two independent experiments with similar results. Actin was used as a loading control. Uncropped blots are available in Supplementary Figure 11.

(**c**) Kaplan-Meier analysis of overall survival of NPM-ALK transgenic mice crossed with WIP deficient mice (Blue, *NPM-ALK/Wip*$^{+/+}$, n = 26; Light blue, *NPM-ALK/Wip*$^{+/-}$, n = 32; Red, *NPM-ALK/Wip*$^{-/-}$, n = 30). The number of mice for each genotype is indicated.

NPM-ALK/Wip$^{+/+}$ *vs NPM-ALK/Wip*$^{+/-}$, ***$P = 0.0044$; *NPM-ALK/Wip*$^{+/+}$ *vs NPM-ALK/WIP*$^{-/-}$, **** $P < 0.0001$; significance was determined by log-rank (Mantel–Cox) test.

(**d**) Western Blot analysis from n = 3 independent primary lymphomas isolated from NPM-ALK transgenic mice crossed with WIP deficient mice. The blot is representative of at least two independent experiments with similar results. Actin was used as a loading control. Uncropped blots are available in Supplementary Figure 11.

(**e**) Representative hematoxylin and eosin stain (left) and immunohistochemistry for Ki-67 (middle) and cleaved Caspase 3 (right), performed on NPM-ALK lymphoma with the indicated genotypes (n = 5 mice for each genotype). Scale bar = 100μm. Insets: high magnification images.

(**f,g**) Quantification of Ki-67 (**f**) and cleaved Caspase 3 (**g**) positive cells in NPM-ALK lymphoma with the indicated genotypes (n = 5 mice for each genotype). Data are shown as means ± s.d.; significance was determined by unpaired, two-tailed Student's t-test.

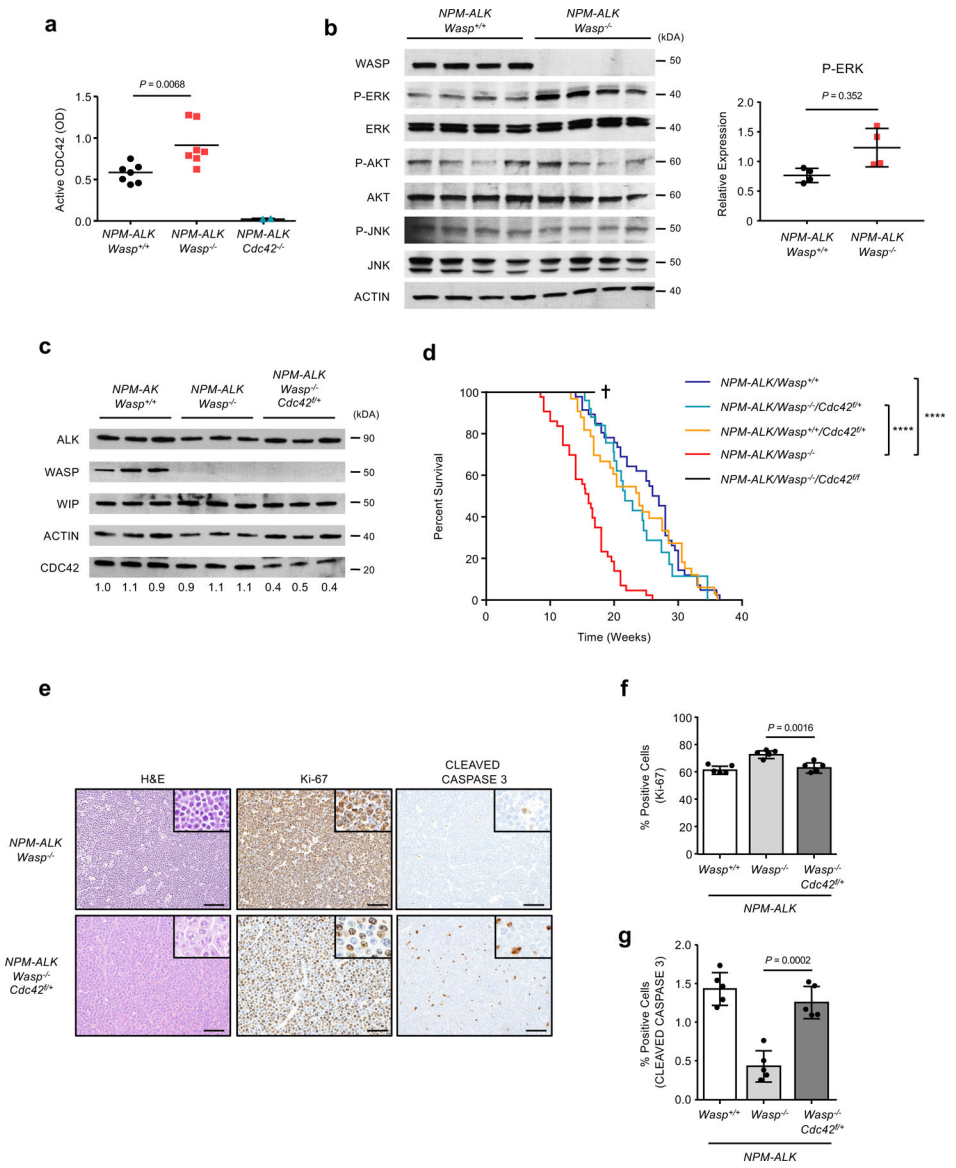

Figure 3. CDC42 and ERK hyperactivation in WASP deficient lymphoma

(**a**) Quantification of active GTP-bound CDC42 using CDC42 G-LISA™ assay kit on cell lines derived from NPM-ALK lymphoma with the indicated genotypes (*NPM-ALK/Wasp*$^{+/+}$ and *NPM-ALK/Wasp*$^{-/-}$, n = 7). *Cdc42* knock-out cell lines (*NPM-ALK/Cdc42*$^{f/f}$*/CD4-Cre* cell lines, n = 2) were used as a control for the assay. Data are shown as means. Significance was determined by unpaired, two-tailed Student's t-test.

(**b**) Western Blot performed with the indicated antibodies on lymphoma cell lines obtained from *NPM-ALK* transgenic (tg) mice with the indicate genotypes (left); quantification of phospho-ERK in lymphoma cell lines (right) (n = 4 biologically independent samples). Data are shown as means ± s.d.; significance was determined by unpaired, two-tailed Student's t-test. Actin was used as a loading control. Uncropped blots are available in Supplementary Figure 11.

(**c**) Western Blot analysis for WASP, WIP and CDC42 expression on the indicated lymphoma cell lines. Densitometric values of the CDC42 bands normalized to actin are indicated. The blot is representative of at least two independent experiments with similar results. Actin was used as a loading control. Uncropped blots are available in Supplementary Figure 11.

(**d**) Kaplan-Meier survival curves of NPM-ALK transgenic mice crossed with *Wasp*$^{+/+}$ or *Wasp*$^{-/-}$ mice with Cdc42 haploinsufficiency (Blue, *NPM-ALK/Wasp*$^{+/+}$, n = 35 mice; Light blue, *NPM-ALK/Wasp*$^{-/-}$*/Cdc42*$^{f/+}$*/CD4-Cre*, n = 24; Red, *NPM-ALK/Wasp*$^{-/-}$, n = 30; Black, *NPM-ALK/Wasp*$^{-/-}$*/Cdc42*$^{f/f}$*/CD4-Cre*, n = 8; Orange, *NPM-ALK/Wasp*$^{+/+}$*/Cdc42*$^{f/f}$*/CD4-Cre,* n = 34). The number of mice for each genotype is indicated. ****P<0.0001; significance was determined by log-rank (Mantel–Cox) test.

(**e**) Representative hematoxylin and eosin stain (left) and immunohistochemistry for Ki-67 (middle) and cleaved Caspase 3 (right), performed on NPM-ALK lymphoma with the indicated genotypes (n = 4 mice for each genotype). Scale bar= 100μm. Insets: high magnification images.

(**f,g**) Quantification of Ki-67 (**f**) and cleaved Caspase 3 (**g**) positive cells in NPM-ALK lymphoma with the indicated genotypes (n = 5 mice for each genotype). Data are shown as, means ± s.d.; significance was determined by unpaired, two-tailed Student’s t-test.

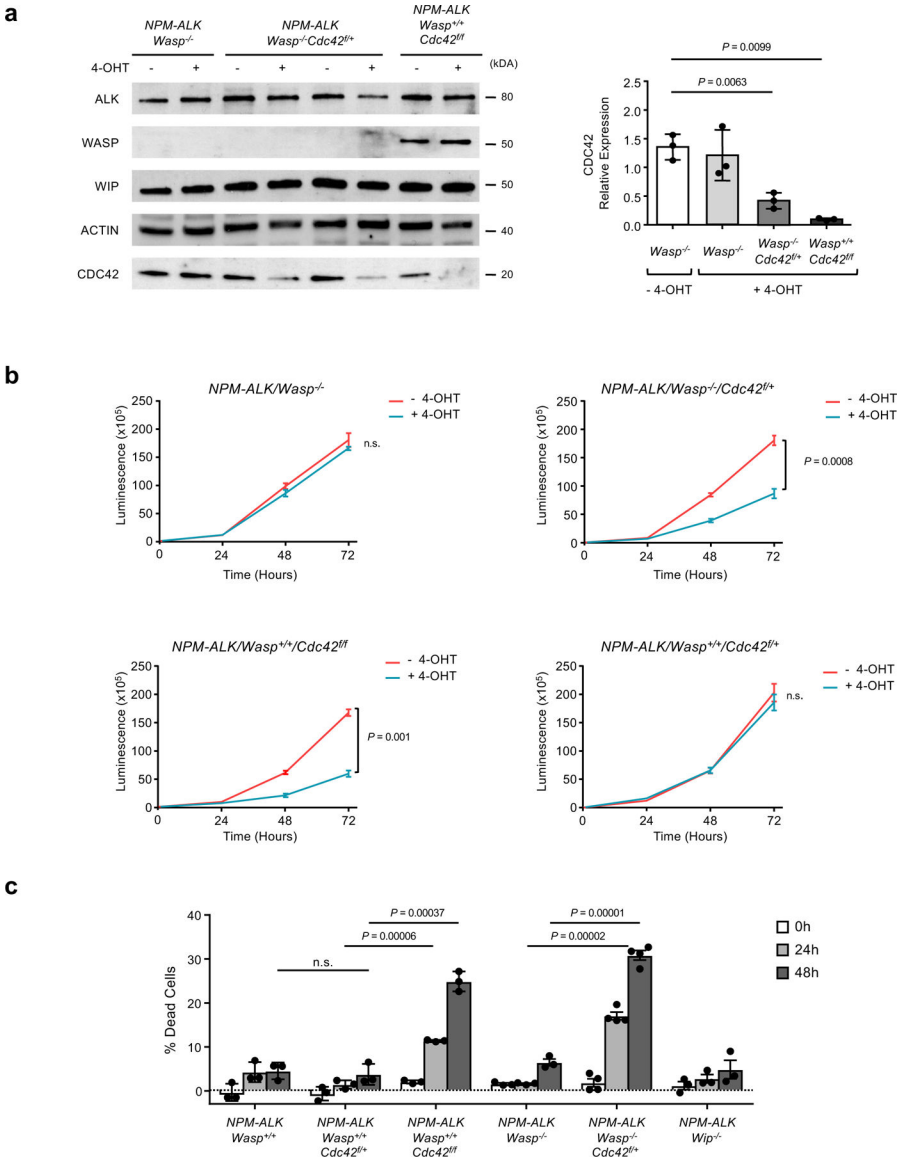

Figure 4. CDC42 is essential for the survival of WASP deficient lymphoma cells

(**a**) Western Blot analysis for ALK, WASP, WIP and CDC42 on lymphoma cell lines obtained from *NPM-ALK* tg mice with the indicated genotypes, transduced with Cre^{ERT2} and treated with 10nM 4-hydroxytamoxifen (4-OHT) for 4 hours (left). The blot is representative of three independent experiments with similar results. Actin was used as a loading control. Uncropped blots are available in Supplementary Figure 11. Mean protein expression of CDC42 in mouse cell lines treated or not with 4-OHT (right). Data are shown as means ± s.d. from 3 independent experiments with similar results; significance was determined by unpaired, two-tailed Student's t-test.

(**b**) Cell growth assay performed on lymphoma cell lines obtained from *NPM-ALK* tg mice with the indicated genotypes, transduced with Cre^{ERT2} and treated with 4-OHT. Measurement has been taken at indicated time points (n = 3 biologically independent

samples). Data are shown as means ± s.e.m.; significance was determined by unpaired, two-tailed Student's t-test; n.s., not significant.

(**c**) Apoptosis analysis performed on lymphoma cell lines obtained from *NPM-ALK* tg mice with the indicated genotypes treated as in (**a**). Measurement has been taken at indicated time points by TMRM staining and flow cytometry analysis. The percentage of dead cells was calculated above background (n = 3 independent experiments). Data are shown as means ± s.d.; significance was determined by unpaired, two-tailed Student's t-test; n.s., not significant.

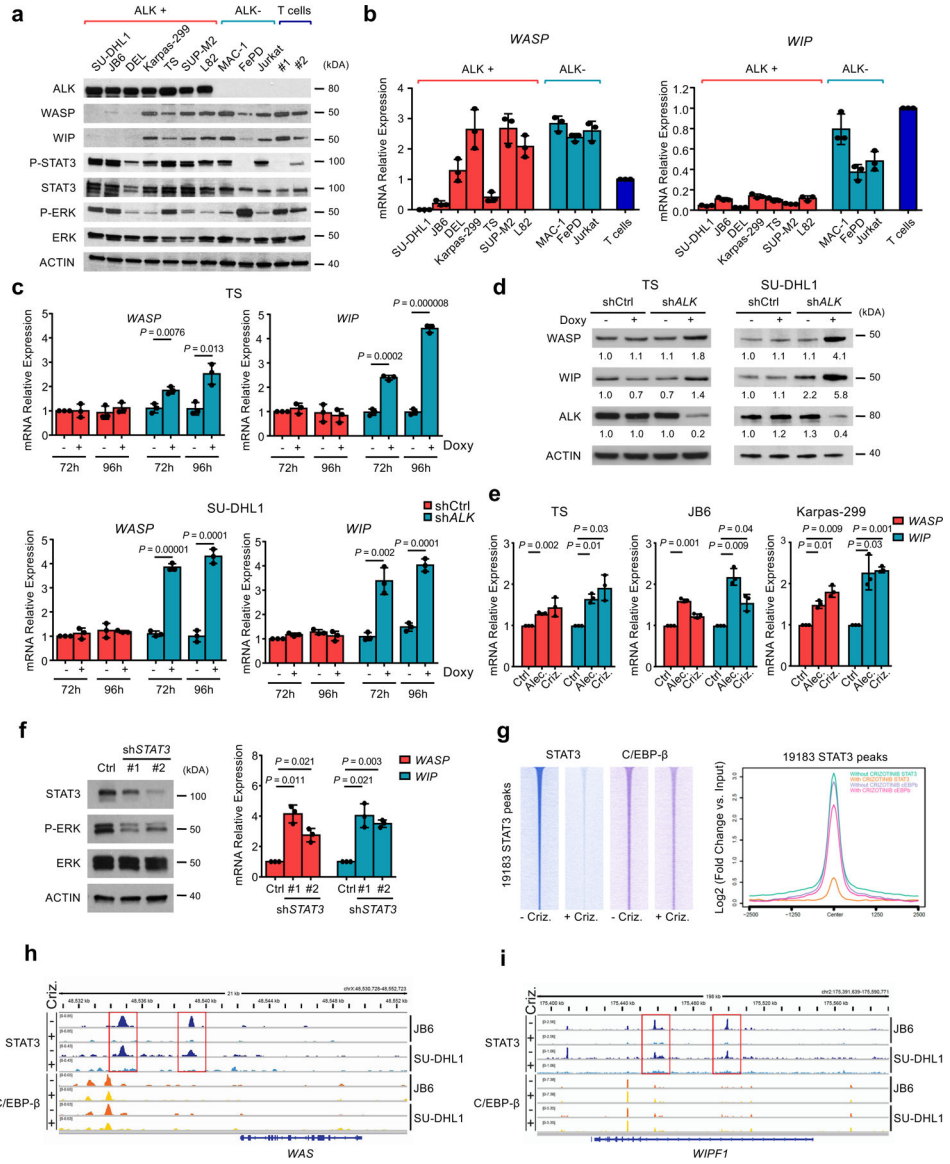

Figure 5. Oncogenic ALK down-regulates WASP and WIP expression through STAT3 and C/EBPβ

(**a**) Western Blot performed on human ALK+ ALCL cells lines and ALK- T lymphoma lines or normal T cells blotted with the indicated antibodies. The blot is representative of two independent experiments with similar results. Actin was used as a loading control. Uncropped blots are available in Supplementary Figure 11.

(**b**) qRT-PCR expression analysis of WASP and WIP mRNA in human ALK+ ALCL cell lines and ALK- T lymphoma lines or normal T cells (n = 3 independent experiments). Data are shown as means ± s.d.

(**c**) qRT-PCR expression analysis of WASP and WIP mRNA on two representative ALK+ ALCL human cell lines (TS and SU-DHL1) transduced with a doxycycline dependent ALK shRNA or control shRNA (n = 3 independent experiments). Data are shown as means ± s.d.; significance was determined by unpaired, two-tailed Student's t-test.

(**d**) Western Blot analysis on the same cells as in (**c**) collected at 96 hours. Densitometric values of the bands are indicated. One representative experiment out of 3 performed is shown. Actin was used as a loading control. Uncropped blots are available in Supplementary Figure 11.

(**e**) qRT-PCR expression analysis of WASP and WIP mRNA on three representative ALK+ ALCL human cell lines (TS, JB6 and Karpas-299) treated with two different ALK inhibitors, alectinib (30 nM) and crizotinib (100 nM) for 12 hours (JB6 and Karpas-299) or 24 hours (TS) (n = 3 independent experiments). Data are shown as means ± s.d.; significance was determined by unpaired, two-tailed Student's t-test.

(**f**) qRT-PCR expression analysis of WASP and WIP mRNA on the ALK+ TS cell line in which the expression of STAT3 has been knocked down by specific shRNA. The corresponding Western Blot of the shRNA KD is shown on the left. Two independent shRNA have been used for each knock-down assay (indicated as #1 and #2). A scrambled shRNA has been used as control (n = 3 independent experiments). Data are shown as means ± s.d.; significance was determined by unpaired, two-tailed Student's t-test. The blot is representative of three independent experiments with similar results. Actin was used as a loading control. Uncropped blots are available in Supplementary Figure 11.

(**g**) Heatmaps (left) and metaplots (right) of global STAT3 peaks obtained by ChIP-seq in SU-DHL1 cells treated for 3 hours with crizotinib (300 nM).

(**h,i**) STAT3 or C/EBP-β ChIP-seq tracks at *WAS* (**h**) and *WIPF1* (**i**) genes on two representative ALK+ ALCL human cell lines (JB6 and SU-DHL1) treated for 3 hours with crizotinib (300 nM). Experiment was performed one time on two independent cell lines with similar results.

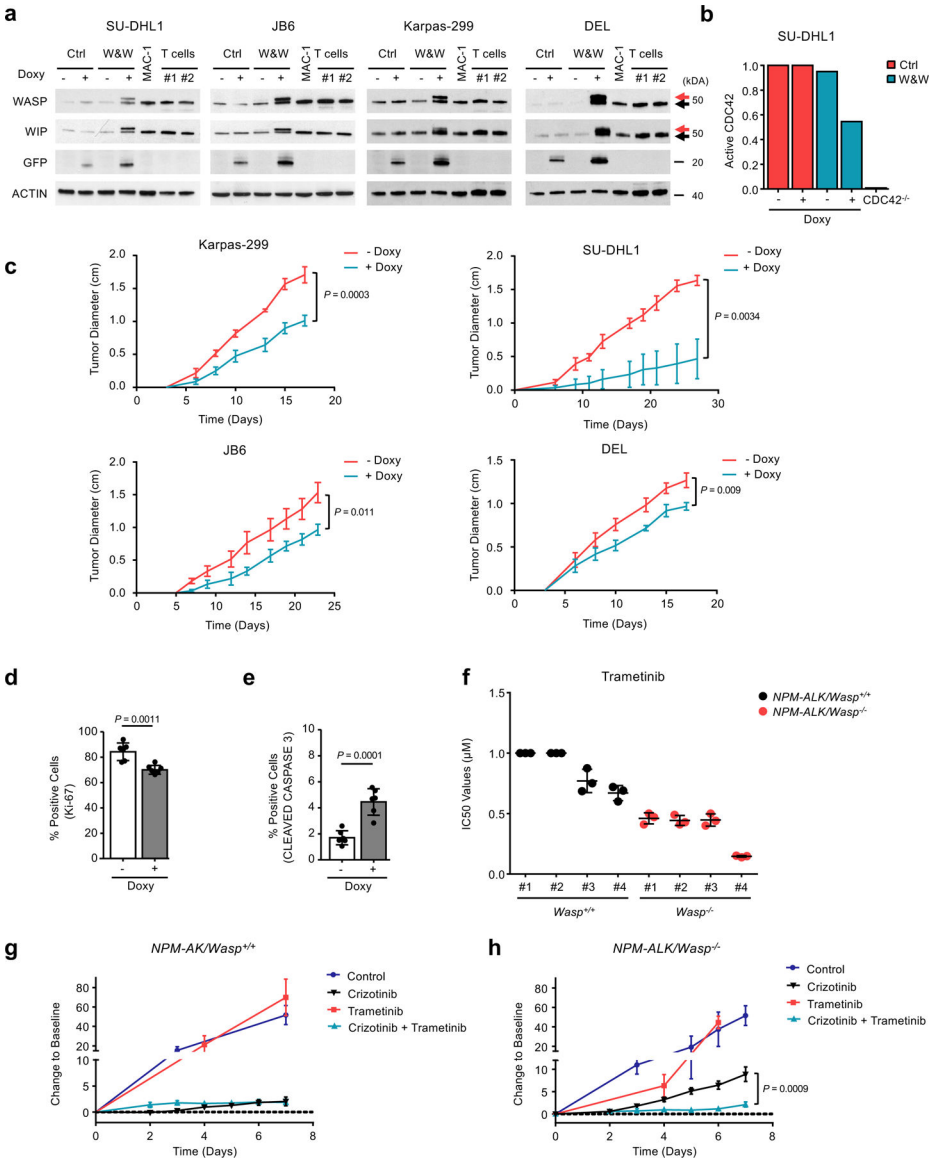

Figure 6. MAPK pathway is a therapeutic vulnerability in WASP-deficient cells.

(**a**) Western Blot analysis of ALK+ ALCL cell lines (SU-DHL1, JB6, Karpas-299 and DEL) transduced with doxycycline-inducible lentivirus co-expressing WASP and WIP (W&W) or a control reporter GFP (Ctrl). Black arrows: endogenous WASP and WIP; red arrows: Flag-tagged WASP and WIP. MAC-1 cell line and normal T cells were used as controls. The blot is representative of at least two independent experiments with similar results. Actin was used as a loading control. Uncropped blots are available in Supplementary Figure 11.

(**b**) Quantification of active GTP-bound CDC42 on SU-DHL1 cell line after induction of WASP and WIP (W&W) expression using CDC42 Activation assay kit CDC42 knockout ($CDC42^{-/-}$) cells were used as a negative control of the assay. One representative of two independent experiments in triplicates is shown.

(**c**) Growth of xenografted tumors in NSG mice injected with ALK+ ALCL cells (Karpas-299, SU-DHL1, JB6 and DEL) transduced with doxycycline-inducible WASP and

WIP (W&W) vectors. Mice were treated with normal (red line) or doxycycline water (light blue line) (n = 6 independent tumors). Data are shown as means ± s.e.m.; significance was determined by unpaired, two-tailed Student's t-test. Doxycycline treatment started at day 0 when cells were injected sub cutis.

(**d,e**) Quantification of Ki-67 (**d**) and cleaved Caspase 3 (**e**) positive cells in ALK+ ALCL xenograft lymphoma as in (**c**) (n = 6 tumors). Data are shown as means ± s.e.m.; significance was determined by unpaired, two-tailed Student's t-test).

(**f**) Sensitivity to trametinib of mouse NPM-ALK lymphoma cells with the indicated genotypes treated for 72 hours with trametinib. Shown are absolute IC50 values (μM, n = 3 biologically independent samples). Data are shown as means ± s.d.

(**g**) Growth of WASP WT or KO NPM-ALK lymphoma cells grafted in NSG mice treated with trametinib alone (1.5mg/kg), crizotinib (30mg/kg) alone or in combination with trametinib (1.5mg/kg). Values shown are the changes in tumor volume from baseline (n = 5 independent tumors). Data are shown as means ± s.e.m.; significance was determined by unpaired, two-tailed Student's t-test.